

1 **An original approach combining biogeochemical signatures and a**
2 **mixing model to discriminate spatial runoff-generating sources in a**
3 **peri-urban catchment**

4
5 Olivier Grandjouan^{1#}, Flora Branger¹, Matthieu Masson¹, Benoit Cournoyer², Nicolas Robinet³, Pauline
6 Dusseux⁴, Angélique Dominguez Lage², Marina Coquery¹

7 ¹ INRAE, UR Riverly, [5 rue de la Doua](#), F-69625, Villeurbanne, France

8 ² Univ Lyon, UMR Ecologie Microbienne (LEM), Université Claude Bernard Lyon 1, VetAgro Sup, France

9 ³ UMR CNRS 5194 Pacte, Université Grenoble Alpes, Cermosem, 1064 chemin du Pradel, 07170 Mirabel, France

10 ⁴ Institut d'Urbanisation et de Géographie Alpine, Université Grenoble-Alpes, CNRS, PACTE, 38100, Grenoble, France

11 *Correspondence to:* Olivier Grandjouan (olivier.grandjouan@insa-lyon.fr)

12 #: present address: INSA Lyon, DEEP, UR7429, 69621 Villeurbanne, France

13 **Abstract.**

14 Hydrograph separation using biogeochemical data is a commonly used method for the vertical decomposition of flow into
15 surface, subsurface and groundwater contributions. However, its application to the spatial decomposition of flow remains
16 limited, despite its potential to identify Such approach is not yet widely used for the spatial decomposition of flow. However,
17 it has great potential for estimating contributions linked to specific geological, pedological, and or land use
18 characteristics, as well as or to particular anthropogenic contaminant sources, in addition to a vertical decomposition. In this
19 study. Aa Bayesian mixing model approach was applied to the Ratier peri-urban sub-catchment of the OTHU Yzeron
20 observatory. Eight runoff-generating sources were identified and sampled, corresponding including to different land uses (e.g.
21 forest, grassland, breeding)agricultural areas, a colluvium aquiferhydrological compartments (e.g. aquifer), and urban point
22 discharges (e.g. sewer system, urban and road surface runoff). A wide range of biogeochemical parameters were analysed
23 including classical (i.e., major chemical compounds, dissolved metals) and innovative tracers (i.e., characteristics of dissolved
24 organic matter-characteristics, microbial indicators). Streamwater samples collected under contrasting hydro-meteorological
25 conditions revealed distinct source signatures and highly variable contributions, with wastewater dominating under dry weather
26 and rapid surface runoff during summer storms. Using these results, we improved a previously designed perceptual
27 hydrological model of the Ratier and Mercier catchments, at the hillslope scale, which highlighted the potential of spatial
28 tracer-based decomposition in addition to classical vertical hydrological separation. More broadly, this study demonstrates the
29 potential of such mixing model, using classical but also more innovative tracers, to provide insights for validating distributed
30 hydrological models and to anticipate the influence of land use, urbanisation, and climate changes on runoff generation. A
31 Bayesian mixing model method was used to decompose streamwater compositions sampled at the outlets of two sub-
32 catchments, under contrasted hydro meteorological conditions. Results showed distinct biogeochemical signatures mostly
33 linked to the land use and the geological compartments. The estimated contributions were contrasted and strongly influenced

34 by the hydro-meteorological conditions. The inferred contributions were used to improve an existing perceptual hydrological
35 model of the Ratier and Mereier catchments, at the hillslope scale. This confirmed the potential of biogeochemical data to
36 discriminate spatial runoff generating sources according to land use, in addition to a more traditional vertical decomposition.

37

38 **Keywords:** runoff-generating sources, fingerprints, spatial decomposition, [OTHU](#), [OZCAR](#), geochemical tracers, Yzeron

39 **1. Introduction**

40 Peri-urban catchments are characterised by contrasting landscapes that can include natural areas (e.g. forests, moorlands),
41 agricultural areas (e.g. crops, grassland) and urban areas (e.g. residential, commercial or industrial areas). These catchments
42 are under considerable pressure from increasing urbanisation, particularly around large cities (Mejía & Moglen, 2010). Peri-
43 urban landscapes are evolving quickly as natural and agricultural areas are decreasing in favour of urban areas (Jacqueminet
44 et al., 2013). [The growing](#) [This increasing urbanisation](#) [presence of anthropogenic contaminants](#) can alter water pathways and
45 [increase transfer of anthropogenic contaminants](#), leading to serious deterioration of surface water and groundwater quality.

46 Sewer overflows are major vectors for a large number of contaminants such as organic matter, organic micropollutants, trace
47 metal elements (e.g. Cu, Ni, Pb, Zn), nutrients or pathogens (Chocat et al., 2001; Lafont et al., 2006; Pozzi et al., 2024; Walsh
48 et al., 2005). Impervious surfaces act as vectors for many contaminants, via rainwater runoff on urban surfaces, such as certain
49 metals (e.g. Cu, Pb, Zn; Charters et al., 2016) or polycyclic aromatic hydrocarbons (Bomboï & Hernandez, 1991), and microbes
50 (Bouchali et al., 2024). Agricultural activities can also bring significant contributions of contaminants in water such as
51 pesticides (Giri & Qiu, 2016), veterinary products (Martins et al., 2019), animal [faecal](#) [faecal](#) contamination (Marti et al., 2017)
52 or nutrients via fertilization (Penuelas et al., 2023). Small catchments ($\sim 10 \text{ km}^2$) are particularly sensitive to the degradation
53 of the surface water quality, as they generally consist of streams close to contaminant sources associated with low dilution
54 capacity (Giri & Qiu, 2016). Effective management of water resources and water quality requires precise knowledge of the
55 water pathways and sources in peri-urban catchments (Gonzales et al., 2009). However, identifying runoff-generating sources
56 and estimating their contribution is difficult, as direct measurement of each contribution is almost impossible (Tardy et al.,
57 2004).

58 Runoff-generating sources are numerous in peri-urban catchments and can be of different kinds due to the diversity of land
59 uses and the presence of artificial elements that divert water such as sewer systems, sewer overflow devices and impervious
60 areas (Birkinshaw et al., 2021; Jankowfsky, 2011). These sources can be defined as hydrological components (e.g. surface
61 runoff, soil water or groundwater flow; Cooper et al., 2000), as specific land uses (e.g. forest, agriculture, urbanized area;
62 Ramon, 2021), or as point contribution (e.g. sewer overflow or wastewater treatment plant outlet; Pozzi et al., 2024). Runoff-
63 generating sources can also be considered as sub-catchments representing a combination of specific geological, pedological
64 and [land use](#) [land use](#) factors (Barthold et al., 2010).

65 It is now recognised that the biogeochemical composition of water can provide information on the contributions of runoff-
66 generating sources, which cannot be deduced from rainfall-runoff dynamics alone (Birkel & Soulsby, 2015). The use of
67 geochemical signatures through a mixing model is now commonly applied to estimate contributions of runoff-generating
68 sources to streamflow (e.g. Burns et al., 2001; Christophersen et al., 1990; Ladouce et al., 2001; Lamprea & Ruban, 2011;
69 McElmurry et al., 2014). To this day, this approach has been applied to estimate contributions from a wide variety of sources
70 such as groundwater flow, subsurface flow and surface runoff (Gonzales et al., 2009; Ladouce et al., 2001), snow and glacier
71 melt (Kumar et al., 2024; Rai et al., 2019; Wellington & Driscoll, 2004), sources of nutrients (Kaown et al., 2023; Verseveld
72 et al., 2008; F. Wang et al., 2024), sources of sediments (James et al., 2023; Klages & Hsieh, 1975; Vale et al., 2022), or to
73 study the impact of different forest management methods on water quality (Fines et al., 2023; Motha et al., 2003). However,
74 this approach has rarely been applied to estimate contributions from both vertical and spatial runoff-generating sources,
75 although it shows~~To this day, this approach is often limited to a vertical decomposition of streamflow according to groundwater~~
76 ~~flow, subsurface flow and surface runoff (Gonzales et al., 2009; Ladouce et al., 2001)~~. However, this method has also a strong
77 potential for spatial decomposition according ~~to~~runoff generating sources linked to the geological, pedological and land use
78 characteristics of the catchment (Nascimento et al., 2023; Liu et al., 2023; Uber et al., 2019). In addition, the use of tracers is
79 often limited to classical geochemical tracers such as stable isotopes, major ions (Singh & Stenger, 2018) or metals (Barthold
80 et al., 2010). Yet, many other biogeochemical parameters show potential for discriminating additional sources, such as the
81 characteristics of dissolved organic matter (Begum et al., 2023; McElmurry et al., 2014; Sun et al., 2024) or microbial
82 parameters (Colin et al., 2020; Marti et al., 2017).

83 The objective of the present study is to identify runoff-generating sources linked to both vertical and spatial characteristics of
84 a small peri-urban catchment (e.g. geology, land use), and estimate their contributions to streamwater in contrasted hydro-
85 meteorological conditions. This approach is based on the creation of a large biogeochemical dataset through the sampling and
86 analysis of runoff water in a catchment, including e~~C~~Classical and innovative tracers we are used as input data for in within the
87 application of a mixing model. This method is applied~~We applied this approach~~ to the Ratier peri-urban catchment, and its
88 nested Mercier sub-catchment, in France, ~~so as to~~ better understand their hydrological behaviour and to identify potential
89 sources of contamination. First, we present the sampling campaigns for runoff-generating sources and streamwater, as well as
90 sample pre-treatment and analysis ~~and the construction of the biogeochemical dataset~~. Second~~Then~~, we describe the
91 characterization of biogeochemical signatures of the sources and their contributions to streamwater obtained ~~through the via~~
92 hydrograph separation. Finally, we discuss ~~assess~~ the evaluation estimated of the constructed signatures and contributions
93 for each source, an evaluation of the estimated contributions, as well as~~then propose~~ a revision of the initial perceptual
94 hydrological model proposed presented by Grandjouan et al. (2023), to provide a better understanding of the Ratier and Mercier
95 catchments hydrological behaviour.

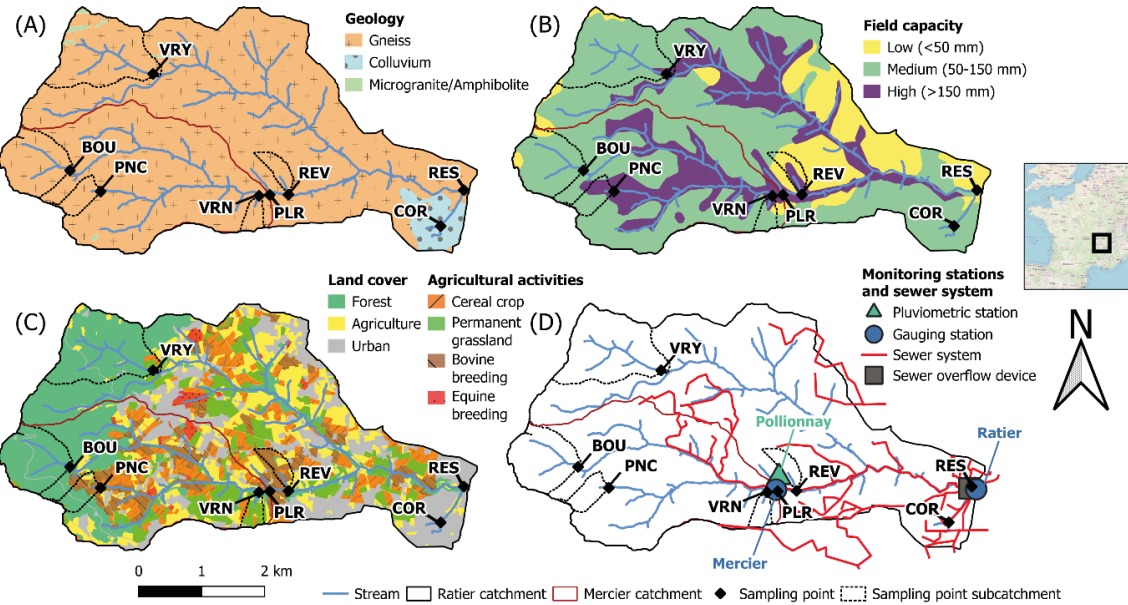
96 **2. Materials and methods**

97 **2.1 Study area:- the Ratier catchment**

98 The Ratier catchment is located west of Lyon, in France. It is part of the Yzeron basin and a site of the Field Observatory in
99 Urban Hydrology (OTHU; <https://www.graie.org/othu/>) and the Critical Zone Observatories: Research and Application
100 OZCAR (<https://www.ozcar-ri.org/>). It covers an area of 19.8 km² and has an altitude ranging between 250 and 780 m. The
101 catchment climate is temperate with [mediterranean](#)[Mediterranean](#) and continental influences (Gnouma, 2006). The bedrock is
102 predominantly crystalline with gneiss underlying 96% of the total surface ([Figure 1](#)[Figure 1](#).A). The shallower part of the
103 gneiss is fractured and provides low perennial groundwater storage (Delfour et al., 1989) The fractured gneiss gradually
104 changes to a weathered clayous-sandy saprolite layer, which varies from less than 1 m thick in the upper part of the catchment
105 to 10 to 20 m in the valley bottom (Goutaland, 2009). The delimitation between this layer and the thin sandy to loamy soils is
106 not clear (Braud et al., 2011). The soils are associated with low to medium field capacities, with the exception of valley bottoms
107 characterised by high field capacities ([Figure 1](#)[Figure 1](#).B). Downstream of the catchment, the eastern part is covered by
108 colluvium deposits holding a local aquifer ([Figure 1](#)[Figure 1](#).A). This catchment is typically peri-urban with 4448% of
109 agricultural areas, 4230% of forest and 4521% of urban areas (Jacqueminet et al., 2013). Field surveys performed by Bétemps
110 (2021) provided information about agricultural activities, which include cereal crop cultures (10% of the catchment area),
111 bovine (10%) and equine breeding (2%) ([Figure 1](#)[Figure 1](#).C). In the urbanized areas, wastewater and rainwater are managed
112 by a combined sewer network and transferred outside the limits of the catchment; however, they can be released in streams
113 during rainstorms via a sewer overflow device located directly upstream of the Ratier outlet ([Figure 1](#)[Figure 1](#).D). The Mercier
114 stream is a tributary of the Ratier stream with a catchment area of 7.8 km². Its geology consists entirely of gneiss bedrock.
115 Land use is predominantly agriculture (4952%) and forest (3842%), with a small proportion of urban areas (513%), including
116 therefore less rainwater drainage facilities than the Ratier catchment.

117 The Pollionnay pluviometric station (Fig. 1.D) records rain and air temperature since 1997. The mean annual precipitation is
118 750 mm and the mean annual minimum and maximum temperatures are 6.6 and 18.4°C from 2010 to 2022 (Grandjouan,
119 2024). Two gauging stations located at the outlets of the Mercier and Ratier catchments allow a continuous hydrological
120 monitoring since 2010 and 1997, respectively ([Figure 1](#)[Figure 1](#).D). Hydrological data show a contrasted hydrological regime,
121 with marked low-flow periods between June and September, particularly upstream where runoff is low throughout the year.
122 The Mercier stream is frequently observed to be dry, unlike the Ratier stream, which is continuously supplied by the colluvium
123 aquifer (Grandjouan et al., 2023). According to the rain and discharge data, the response time (i.e., the time elapsed between
124 the peak of rainfall and the corresponding peak in discharge) for the Ratier catchment is around 30 minutes.

125



126
127 **Figure 1** – Maps of the Ratier and Mercier catchments showing the sampling points (see [Table 1](#) for details) and (A) geology
128 (David et al., 1979; Delfour et al., 1989; Gnouna, 2006), (B) field capacity (Labbas, 2014), (C) land use (Jacqueminet et al., 2013)
129 and agricultural activities (Bétemp, 2021) and (D) monitoring stations and sewer system (from Grand Lyon and SIAHVY).

130

131 2.2 Field data acquisition

132 2.2.1 Source identification and sampling

133 In this study, we mainly considered runoff-generating sources as homogeneous sub-catchments associated with a combination
134 of representative factors including geology, field capacity, land use, and agricultural activities, and the sewer. We based our
135 work on the two hypotheses: (1) that the biogeochemical composition of streamwater at the outlet of these each sub-
136 catchments is representative of these its associated factors (Barthold et al., 2010); and (2) the runoff contributions from a
137 specific source is proportional to its spatial extent within the catchment.

138 The first step in identifying these sources involved the superposition of geological, field capacity, land use and agricultural
139 activities maps (Figure 1). This allowed us to obtain determine which combinations of factors are In this way, we
140 identified the most spatially representative combinations of factors most spatially represented in the catchment, as detailed in
141 Table A1 shows the relative areas corresponding to each combination obtained. Based on these results, we identified the main
142 sources and named them according to their associated land use: forest (FOR), grassland (GRA), agriculture (AGR), colluvium
143 aquifer (AQU), and urban and road surface runoff from impervious areas (URB) (see Table 1). We considered quick surface
144 runoff from other areas (SUR) as an additional source, resulting from infiltration excess or saturation excess overland flow
145 (Beven, 2012). A last source We identified is wastewater (SEW) as a last source that, which can be transferred discharged

146 from the combined sewer system into the stream via through an overflow device located downstream of the Ratier catchment
147 (Figure 1.D), or other overflow pipes. Table 1 provides a description of the factors corresponding to these sources, the main
148 combinations of factors existing in the catchment.

149 Then, We then selected sampling points where representative of samples could be taken from each source. These points are
150 located .We selected Sampling points are selected at the outlet of several selected sub-catchments (Table 1Table 1 and Figure
151 1Figure 4), according to the predominantly represented combinations of factors as well as and a field reconnaissance surveys,
152 which allowed to check the consistency of the data and use, particularly for agricultural activities, which that may evolve from
153 year to year. The presence of even a permanent small flow, even a weak one, at the sub-catchments outlets was also a
154 requirement for the sampling points selection. The localisation of each sampling point is illustrated in Figure 1Figure 1. We
155 selected the colluvium groundwater sampling point (COR) in the upstream section of a stream draining this aquifer. In the case
156 of forest FOR and grassland GRA sources, we selected two sampling points are selected for each source to compare the
157 biogeochemical signatures obtained from two sub-catchments of the same type (i.e., BOU and VRY, VRN and REV,
158 respectively). As no homogeneous sub catchment could be identified for single agricultural activities, an The agricultural sub-
159 catchment (PNC) includinges bovine breeding and cereal crops is preferred. The colluvium groundwater sampling point (COR)
160 is chosen in the upstream section of a stream draining this aquifer. Two distinct runoff generating sources associated to surface
161 runoff are considered: (1) urban and road surface runoff from impervious areas, and (2) quick surface runoff from other areas
162 resulting from infiltration excess or saturation excess overland flow (Beven, 2012). For the first type of the URB runoff, we
163 selected a storm water discharge point (PLR) fed by runoff from a road and an upstream urban area is selected. For the second
164 typeSUR runoff, we chose planned to collect sample sampling of didi rect surface runoff during rainfall events, directly from
165 the surface of forest and agricultural sub-catchments (BOU, VRY, REV and PNC) is selected. In order to approach sewer
166 system overflow condition, wWe sampled collected An additional source is wastewater, which can be transferred from the
167 combined sewer system to the stream through an overflow device located downstream the Ratier catchment (Fig. 1.D), or other
168 overflow pipes. Sampling of wastewater is chosen directly in the sewer system (RES) during rainy period periods of rainfall,
169 to approach a sewer system overflow situation.

170 **Table 1 – Identified runoff-generating source sources and corresponding Selected sampling points with for runoff generating**
 171 **sources and their relative sub-catchments areas, geology, field capacity, land use and main features, based on information**
 172 **provided in Figure 1Figure 1 and field observations. n.a. : non available**

Source		Sampling point	Sub-catchment area (ha)	Geology	Field capacity ¹	Land use (%) and main features		
Code	Description					Forest	Agriculture	Urban
AQU	Colluvium aquifer	COR	-	-	-	-	-	-
FOR	Gneiss / Medium field capacity / Forest	BOU	88	Gneiss	Medium	Deciduous, coniferous	100	- 0 - 0
		VRY	151	Gneiss	Medium	Deciduous, coniferous	100	- 0 - 0
GRA	Gneiss / Medium to high field capacity / Grassland	VRN	13	Gneiss	Medium	Decidous	30	Grassland 70 - 0
		REV	18	Gneiss	Low to high	Decidous	30	Grassland 70 - 0
AGR	Gneiss / Medium field capacity / Agriculture	PNC	22	Gneiss	Medium to high	-	40	Grassland, bovine breeding, cereal crop 25 Landfill 15
URB	Urban and road surface runoff	PLR	-	-	-	-	-	-
SUR	Quick surface runoff	n.a.	-	-	-	-	-	-
SEW	Sewer system	RES	-	-	-	-	-	-

¹ Among low, medium and high field capacities identified by Labbas (2014).

Sampling point		Sub-basin area (ha)	Geology	Field capacity ¹	Land use (%) and main features		
Site/Source	Code				Forest	Agriculture	Urban
Bouillon stream	BOU	88	Gneiss	Medium	Deciduous, coniferous	100	- 0 - 0
Verdy stream	VRY	151	Gneiss	Medium	Deciduous, coniferous	100	- 0 - 0
Varennes	VRN	13	Gneiss	Medium	Decidous	30	Grassland 70 - 0
Le Revay	REV	18	Gneiss	Low	Decidous	30	Grassland 70 - 0
Ponce	PNC	28	Gneiss	Medium	-	40	Grassland, bovine breeding, cereal crop 25 Landfill ² 15
Corlevet spring	COR	-	-	-	-	-	-
Wastewater	RES	-	-	-	-	-	-
Urban and road runoff	PLR	-	-	-	-	-	-
Quick surface runoff	-	-	-	-	-	-	-

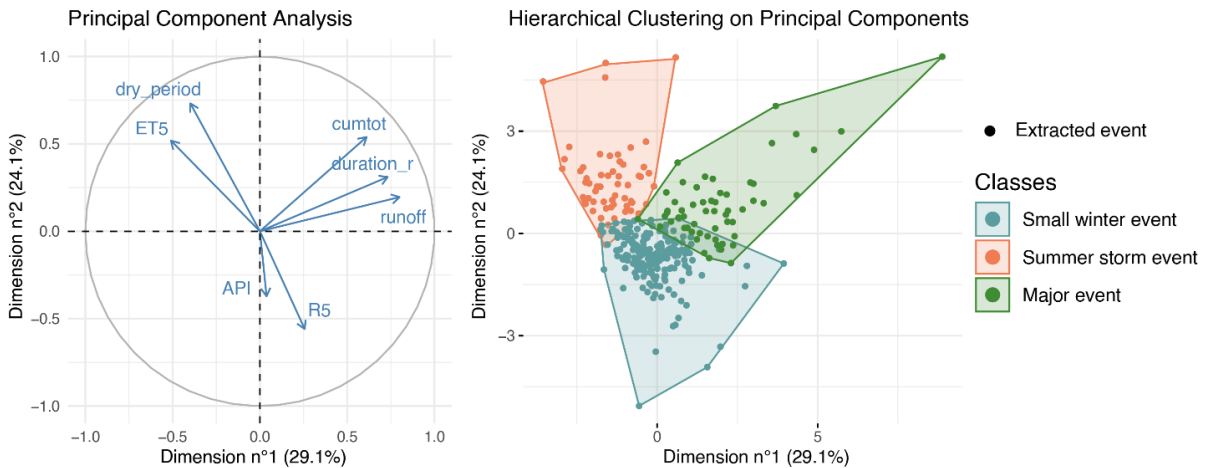
¹ Among low, medium and high field capacities identified by Labbas (2014).

² Soils displaced from urban building sites

175
176 In order to assess the seasonal variability of the biogeochemical water composition, ~~sources are sampled~~we sampled sources
177 in contrasted hydro-meteorological conditions. ~~We considered~~ Low flow conditions ~~are considered~~ from June to September,
178 and high flow conditions from October to May. ~~We considered~~ Wet weather conditions ~~are considered~~ when the cumulative
179 rain over 5 days exceed~~sed~~ 3 mm, and dry weather when it ~~is was~~ below 3 mm, this value being the median of daily rainfall
180 recorded between 2011 and 2023 at the Polionnay station. ~~We performed~~ Eight source sampling campaigns ~~were carried out~~
181 between February 2022 and March 2023. ~~We collected~~ Four to 5 water samples ~~were collected~~ manually in sampling bottles
182 for each sampling point, for a total of 38 source samples.
183 Some field observations differed from the initial information provided in Figure 1~~Figure 1~~. ~~No~~ bovine breeding was observed
184 at REV during the campaigns, whereas cereal crops were observed at PNC. ~~No~~ direct surface runoff was observed during
185 the campaigns at BOU, VRY, VRN and REV. ~~as a consequence, so we could not sample~~ the ~~quick surface runoff~~SUR source
186 could not be sampled.

187 2.2.2 Streamwater sampling during hydrological events

188 We also sampled streamwater at the outlets of the Mercier and Ratier catchments, targeting contrasted hydrological events. To
189 do so, ~~we extracted~~ past hydrological events ~~were extracted~~ from the data available for years 2011-2021, and analysed them
190 following the approach presented by ~~Braud et al., (2018)~~Braud et al. (2018). ~~We calculated~~ Seven hydro-meteorological
191 indicators ~~were calculated~~ to characterise the 315 extracted events, namely: duration of rain, cumulative rainfall, total runoff,
192 5-day cumulative reference evapotranspiration, dry period duration, antecedent precipitation index, and 5-day cumulative
193 rainfall (Figure 2~~Figure 2~~). Based on a Hierarchical Clustering Analysis (HCA), the events were classified according to ~~the~~se
194 indicators. ~~We identified an optimal number of three classes using the “elbow” method~~ (Thorndike, 1953); ~~then, and~~
195 ~~associated~~assigned a class to the ~~them to~~ Three classes of hydrological events were identified ~~different types of events~~: small
196 winter events, summer storm events and major events. Figure 2~~Figure 2~~ shows a Principal Component Analysis (PCA)
197 visualisation of this classification. Major events are defined by high precipitation rate, long duration and high total runoff
198 volume. Summer storm events are characterised by a long dry period before the beginning of the event and high
199 evapotranspiration rate. Small winter events represent the majority of the extracted events (63%) and are characterised by low
200 values for all the indicators. Antecedent precipitation index (API), which corresponds to the sum of daily precipitation weighted
201 according to a multiplying factor ($k = 0.8$;~~Sarrazin, (2012)~~), and the cumulative rainfall 5 days (R5) before the event, did
202 not mark any specific event class. Based on this classification, we defined a sampling objective of two hydrological events by
203 class to study intra-class variability and taking in account the difficulty to ~~of~~ targeting major and summer storm events.events
204



205
 206 **Figure 2 – Principal Component Analysis visualisation of the hydrological event classification based on a Hierarchical Clustering**
 207 **Analysis.** *duration_r*:- duration of raining event; *cumtot*:- cumulative rain during the event; *runoff*:- total runoff during the event;
 208 *ET5*:- cumulative reference evapotranspiration 5 days before the event; *dry_period*:- duration of dry period before the event; *API*:-
 209 *antecedent precipitation index at the beginning of the event*; *R5*:- cumulative rain 5 days before the event.

210

211 We used auAutomatic samplers (Endress+Hauser Liquiport CSP44) were used to sample streamwater at the Mercier and Ratier
 212 gauging stations (Figure 1Figure 1). We carried out Aa weather alert monitoring was carried out to launch the sampling
 213 campaigns according to the targeted hydrological events. We adapted Sampling time steps were fixed and adapted to each
 214 event, from 10 to 45 minutes, according to the expected duration of the rain. Six hydrological events were sampled between
 215 March 2019 and March 2023, ensuring two events per class. The March 2019 and June 2022 events were not sampled at the
 216 Ratier and Mercier station, respectively, due to technical issues on the automatic samplers. We obtained Twenty20 to 24
 217 samples were obtained for each event, and mixed them two by two in order to ensure sufficient volume for analysis. After
 218 pairing, 10 to 12 samples were finally obtained for each event and at each gauging station. Table 2Table 2 shows the hydro-
 219 meteorological indicators calculated for these events.

220

221

Table 2 – Hydro-meteorological indicators calculated for the hydrological events sampled at the Mercier and Ratier gauging stations. The Sampled station column indicates at which gauging station the event was sampled. duration_r: duration of raining event; cumtot: cumulative rain during the event; runoff: total runoff during the event; ET5: cumulative reference evapotranspiration 5 days before the event; dry_period: duration of dry period before the event; API: antecedent precipitation index at the beginning of the event; R5: cumulative rain 5 days before the event.

Event sampling campaign	duration_r (h)	cumtot (mm)	runoff (mm)	ET5 (mm)	dry_period (h)	API (mm)	R5 (mm)	Event class	Sampled station
06/03/2019	20	7	0.3	8	55	0	3	Small winter event	<u>Mercier</u>
10/05/2021	44	92	11.6	13	70	0	10	Major event	<u>Mercier/Ratier</u>
03/10/2021	80	89	5.8	13	147	0	0	Major event	<u>Mercier/Ratier</u>
22/06/2022	116	57	0.3	38	291	0	0	Summer storm event	<u>Ratier</u>
14/09/2022	44	9	0.1	15	94	0	2	Summer storm event	<u>Mercier/Ratier</u>
13/03/2023	19	18	0.7	7	13	1	27	Small winter event	<u>Mercier/Ratier</u>

229 2.2.3 Streamwater sampling during dry weather

230 We also considered Streamwater composition was also considered at dry weather. Data used come from an available dataset
231 described in Grandjouan et al. (2023). In this latter study, monthly monitoring campaigns were conducted from March 2017
232 to December 2019 at the outlets of the Mercier and Ratier catchments. and a total of 24 samples were collected manually.
233 These samples were classified into low flow (June to September) and high flow (October to May) conditions.

234 2.2.4 Sample pre-treatment and analysis of biogeochemical parameters

235 All source and streamwater samples were filtered at 0.45 µm and analysed for a set of 35 44 biogeochemical parameters in
236 order to obtain a more accurate characterisation and discrimination of the identified sources. This list includes geochemical
237 parameters, characteristics of the dissolved organic matter (DOM), and two microbial parameters (Table 3). Classical tracers
238 like major ions, silica and trace elements were selected as they can be closely related to geological characteristics of the
239 catchments, particularly Ca²⁺, SiO₂ and Sr for crystalline formations like gneiss (Fröhlich, Breuer, Frede, et al., 2008; White
240 et al., 1999). They can also be helpful to trace the contribution of agricultural activities as K⁺ (Cooper et al., 2000), Cd (El
241 Azzi et al., 2016), Cu (Vian, 2019) or As (Yokel & Delistrat, 2003). Trace metals can trace urban origin of water, as for Cd,
242 Cr, Cu, Ni, Pb, Rb or Zn (Becouze-Lareure, 2010; Coquery et al., 2011; Froger et al., 2020; Lamprea & Ruban, 2011). Finally,
243 major ions such as K⁺ and Na⁺ can be observed at high concentrations in wastewater (Fröhlich et al., 2008). We selected UV-
244 Visible and HPSEC indicators as they can represent both natural and anthropogenic sources by characterising the molecular
245 weight of DOM. The spectral slope S1 is inversely correlated with this molecular weight and high S2 values are more likely
246 to be associated with terrestrial MOD, compared to fresh algal MOD (Helms et al., 2008). The HPSEC indicators A0, A1, A2
247 and A3 represent very large, large, small and very small molecules, respectively (Boukra et al., 2023). We selected the HF183

248 and *rum-2-bac* host-specific microbial DNA targets to detect and trace faecal contamination from human and ruminant,
249 respectively.

250 including geochemical parameters, characteristics of the dissolved organic matter (DOM), and ~~two~~ two microbial parameters
251 (Table 3). Additional parameters were analysed for these samples but not used in ~~these~~ the present study. The full set of 55
252 biogeochemical parameters is available at : <https://entrepot.recherche.data.gouv.fr/dataverse/chypster/> (Masson et al., 2025a,
253 2025b).

254 Geochemical parameters included ~~610~~ 610 major ions, silica and ~~1547~~ 1547 trace metal elements. Major ions were analysed by ion
255 chromatography, silica by colorimetry and trace elements by inductively coupled mass spectrometry (ICP-TQ-MS). The
256 absence of contamination was systematically verified by the analysis of blanks. ~~limits~~ Limits of quantification (LQ) and analytical
257 uncertainties are detailed in Table A2-Table A1. The accuracy and uncertainties of the methods were routinely checked using
258 certified standard solutions and reference materials, as well as regular participation in interlaboratory testing.

259 Characteristics of the DOM included Dissolved Organic Carbon (DOC) ~~and total dissolved nitrogen (DTN)~~ concentrations,
260 ~~82~~ two Ultra Violet-Visible (UV-Vis) indicators and ~~5~~ five 7 High Pressure Size Exclusion Chromatography (HPSEC)
261 indicators. The DOC ~~and DTN~~ analyses were performed by high temperature catalytic combustion. The UV-Vis indicators
262 were calculated from absorbance spectra obtained between 200 and 800 nm from UV-Visible spectrophotometry analyses, as
263 described by Li & Hur (2017) and Boukra et al. (2023). The HPSEC analyses were performed as described by Boukra et al.
264 (2023) and HPSEC indicators were calculated from chromatogram obtained with UV detection at a wavelength of 254 nm
265 according to Peuravuori & Pihlaja (1997).

266 Microbial parameters included ~~7~~ two host-specific microbial DNA targets, ~~markers of~~ human faecal bacterial contamination
267 (*HF183* DNA target) and ruminant contamination (*rum-2-bac* DNA target). Targets were tracked ~~tracked~~ using a quantitative
268 Polymerase Chain Reaction method (qPCR). The DNA extraction~~s~~ were performed as indicated in Pozzi et al. (2024) ~~and~~.
269 The qPCR assays ~~for~~ human (*HF183* DNA target) and ruminant (*rum-2-bac* DNA target) fecal bacterial tracers, and ~~for tracking~~
270 ~~classes 1 and 2 integrons~~ PCR assays ~~were~~ performed according to Bouchali et al. (2024).

271

272 ~~Integrons are genetic shuttles that can encode antibiotic resistances, biocide degradation genes, and other functional genes
273 involved in quick adaptive processes (e. g. Colinon et al., 2010).~~

274

275 **Table 3 – Measured biogeochemical parameters and respective analytical methods. The tracers in bold correspond to reductionist
276 the final selection of tracers used in the mixing model (see Section 3.2). Measured biogeochemical parameters and respective
277 analytical methods**

Parameter family	Biogeochemical parameter	Biogeochemical parameter	Analytical method	Analytical method
Major anions	Cl^- , SO_4^{2-}	Cl^- , SO_4^{2-} , NO_3^- , NO_2^- , PO_4^{3-} , SO_4^{2-}	Ionic chromatography	NF EN ISO 14911 (1999)
Major cations	Ca^{2+} , K^+ , Mg^{2+} , Na^+	Ca^{2+} , K^+ , Mg^{2+} , Na^+ , NH_4^+	Ionic chromatography	NF EN ISO 10304-1 (2009)

<u>Silica</u>	<u>SiO₂</u>	Colorimetry NF T 90-007 (2001)
Dissolved metals	<u>Al, As, B, Ba, Cd, Co, Cr, Cu, Li, Mo, Ni, Pb, Rb, Sr, Ti, U, V, Zn</u>	ICP-MS
Dissolved organic carbon and dissolved nitrogen	<u>Al, As, B, Ba, Cd, Co, Cr, Cu, Fe, Li, Mn, Mo, Ni, Pb, Rb, Sr, Ti, U, V, Zn</u> <u>DOC, DTN</u>	NF T 90-007 (2001) <u>Catalytic combustion</u> <u>NF EN 1484</u>
Dissolved organic carbon	<u>DOC</u>	<u>Dosage</u> <u>NF EN 1484</u>
UV-Visible indicators	<u>E2:E3, E2:E4, E3:E4, E4:E6, S1, S2, SR, SUVA</u>	<u>UV-visible spectroscopy</u> <u>UV-visible spectroscopy</u>
HPSEC indicators	<u>Mn-254, A0-254, A1-254, A2-254, A3-254</u>	<u>High Pressure Size Exclusion Chromatography</u>
HPSEC indicators	<u>Mn-254, Mw 254, disp 254, A0 254, A1 254, A2 254, A3 254</u>	<u>High Pressure Size Exclusion Chromatography</u>
Microbial qPCR assays	<u>Total bacteria (G16S), total Bacteroidales (BT),</u> <u>#Human marker Bacteroides (HF183), ruminant marker Bacteroides (rum-2-bac), sewer system marker (BTS),</u> <u>classes 1 and 2 integrans</u>	qPCR

278

279 **2.2.5 Quick surface runoff from non-urban areas**

280 As no surface runoff could be sampled for the SUR source, we considered that the biogeochemical composition of quick
 281 surface runoff away from impervious areas was close to the composition of rainwater, assuming that it does not have enough
 282 time to acquire significant biogeochemical elements from the soil it flows over. Such hypothesis is supported by the
 283 concentrations of several parameters in streamwater during rainy weather (e.g. Cl⁻, SO₄²⁻, SiO₂, Mg²⁺, Na⁺), which are lower
 284 than all concentrations measured in the source samples. This observation suggests dilution by low-mineralised inputs.
 285 However, this assumption does not take into account the enrichment of water by soil leaching. Therefore, we examined final
 286 results will be examined considering that this assumption may lead to an underestimation of the quick surface runoff
 287 contribution when applying the mixing model for hydrological events (see Sections 4.1 and 4.2). Therefore, the SUR
 288 source (SUR) is was then associated to rainwater biogeochemical composition obtained from at the Polionnay pluviometric
 289 station (Figure 1Figure 1; Lagouy et al., 2022), sampled between 2017 and 2023, for major ions, DOC and UV-Vis indicators
 290 (n = 9). We used Data from the Ecully pluviometric station (10 km from Polionnay) is used for trace metal element
 291 concentrations, produced by (Becouze-Lareure, 2010) between 2008 and 2009 (n = 32). No data is was considered available
 292 for HPSEC and microbial indicators for the quick surface runoff source.

293

294 **2.3 Characterization and biogeochemical signatures of runoff-generating sources**

295 **2.3.1 Biogeochemical composition and typology of runoff-generating sources**

296 All data obtained from the 388 source water samples and the 5235 analysed parameters ~~were~~ used to provide a detailed global
297 characterization of the biogeochemical composition for each source. This description ~~is~~was used to compare the
298 biogeochemical composition of the identified sources, as well as to study their variability according to the hydro-
299 meteorological conditions, in order to confirm similarities, and thus the grouping of samples collected from the same type of
300 source (BOU and VRY for forest; VRN and REV for agriculturegrasslands) or, on the contrary, the distinction between groups
301 of samples. We used aA Hierarchical Clusteringassification Analysis (HCA) is used to classify the samples according to the
302 biogeochemical dataset and to create a typology of sources. We applied HCA based on an optimal number of class determined
303 with the “elbow” method (Thorndike, 1953), using absolute concentrations that we centred and scaled. The purpose of this
304 typology is to describe the nature of the sources that will be considered in the mixing model.

305 **2.3.2 Building-up the biogeochemical signatures**

306 A biogeochemical signature can be defined as a limited selection of discriminating and representative tracers. (Fröhlich, Breuer,
307 Frede, et al., 2008; White et al., 1999)(Fröhlich, Breuer, Frede, et al., 2008; F. Liu et al., 2008)(Cooper et al., 2000)(El Azzi
308 et al., 2016)(Vian, 2019)(Yokel & Delistraty, 2003)trace(Coquery et al., 2011; Fröger et al., 2020; Lamprea & Ruban, 2011;
309 Froger et al., 2020)such (Fröhlich, Breuer, Frede, et al., 2008)(Helms et al., 2008)The , respectively(Boukra et al.,
310 2023)(Reischer et al., 2006)(Seurinck et al., 2005) Using selected tracers, we built biogeochemical signatures that fed a mixing
311 model to estimate the contribution of sources at the catchment outlet.with the selected tracers from which it is possible to
312 apply a mixing model approach to estimate the contribution of sources at the catchment outlet. The tracers used in a mixing
313 model must be additive, conservative and discriminating. (Christophersen & Hooper, 1992; Tiecher et al., 2015)and must be
314 considered as conservative through the mixing process (Christophersen & Hooper, 1992; Stock et al., 2018; Tiecher et al.,
315 2015) (see, sSection 2.4 providesfor more details on the assumptions required when applying a mixing model). To build these
316 biogeochemical signatures, We applyeda reductionist tracerss selection approach based on the biogeochemical dataset for
317 5235 parameters. This approach aimed at
318 selecting the smallest combination of tracers showing the highest inter-source variability and the lowest intra-source variability.
319 All major parameters and metals ~~are~~were considered additives regarding their chemical characteristics (Benjamin, 2014). The
320 bacterial DNA targets ~~Non additive UV Vis (E2:E3, E2:E4, E3:E4, E4:E6, SUVA, SR) and HPSEC indicators (Mw 254,~~
321 ~~disp~~254) are eliminated according to laboratory tests performed by Baduel (2022). Conservative (HF183HF183 and rum-2-
322 bac and ruminant Bacteroides DNA markers) and non-conservative (integrons, 16S rRNA rrs gene, Bacteroidales DNA
323 marker) bacterial DNA targets show undefined relations with abiotic parameters, which prevent their use in a mixing model.
324 Although we discarded them from the reductionist tracer approach, we used them afterwards to evaluate the biogeochemical
325 signatures and the estimations obtained.

326 We eliminated are used in this investigation, but their undefined relations with abiotic parameters led to their removal from
327 the parameter list for this particular task. Phosphates (PO₄³⁻), nitrogen compounds (DTN, NO₃⁻, NO₂⁻, NH₄⁺), Fe and Mn are
328 considered too reactive and therefore non-conservative. Other non-conservative parameters are eliminated by applying a
329 range-test method (Sanisaca et al., 2017; Wilkinson et al., 2013), that check that the concentrations measured in a mixture
330 (here the streamwater sampled at the Mercier and Ratier outlets during the hydrological events) are comprised within the limits
331 represented by the concentrations observed in the source samples. Failure of this test suggested a non-conservative parameter
332 or a missing source (Collins et al., 2017). We then eliminated Non-discriminating parameters are eliminated using a Kruskal-
333 Wallis test (Kruskal & Wallis, 1952) followed by a Dunn post hoc test (Dunn, 1964), with a p-value threshold of 0.05. The
334 null hypothesis is that the distributions of each parameter are identical across all groups; parameter for which this hypothesis
335 could not be rejected are considered non-discriminating. Lastly, we selected the most discriminating tracers are selected using
336 a Linear Discriminant Analysis (LDA) coupled to a Wilks lambda approach (Collins et al., 1997). We used This method is
337 used to select the smallest combination of tracers showing the highest inter-source variability and the lowest intra-source
338 variability. The remaining tracers are used to build the biogeochemical signatures of the runoff-generating sources, in the
339 form of radar plots, using min-max standardized concentrations to obtain values between 0 and 1.

340

341 2.4 Estimation of the source contributions at the outlet of the catchments

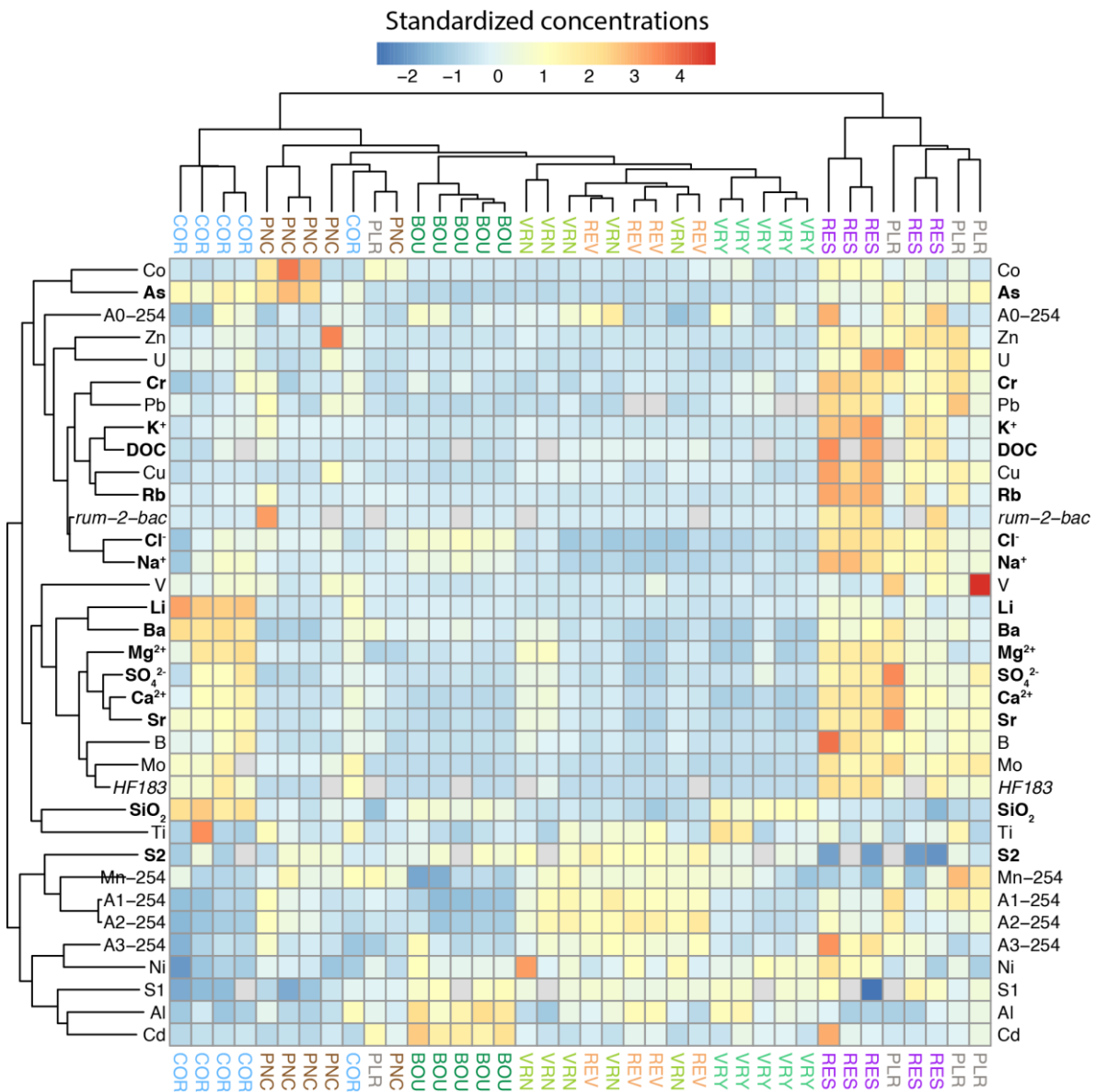
342 We applied aA mixing model is applied to decompose streamwater for samples collected at the Ratier and Mercier sub-
343 catchment outlet stations. We respected the basic assumptions when applying a mixing model provided by(Stock et al., 2018),
344 suggesting that a user must verify that : (1) all sources which contributes to streamwater are identified, (2) the signature from
345 source to the mixture is not altered (see Section 2.3.2), (3) the source signatures are fixed, (4) the contributions sum to 100%
346 and the signature of sources differ. We estimated the source contributions during dry weather, and during the 6six targeted
347 hydrological events. In the absence of rain, we did not consider urbann and road surface runoff and, as well as quick
348 surface runoff are not considered as sources contributing to the streamwater samples. (Stock et al., 2018)(Stock et al., 2018) We
349 chose a Bayesian approach to resolve the mixing model equations, using the package *MixSIAR* in R (Stock et al., 2018), this
350 approach allowing for the incorporation of uncertainty in both source and mixture data. The prior information chosen for
351 source contributions, representing the initial assumption about the relative contributions of each source, correspond to $1/n$,
352 where n is the number of sources considered. The prior information on the biogeochemical parameter concentration for the
353 sources, representing the initial assumption about these concentrations, is was modelled as a normal distribution, defined by
354 the mean and covariance matrix of the measured concentration.

355 As indicated above, As a prior hypothesis, we expected the contributions from each source to be proportional to their spatial
356 extent, with the exception of wastewater. Results that would invalidate this assumption hypothesis would suggest the influence
357 of additional factors beyond the spatial extent of catchment characteristics, such as differences in vertical flow transfer,
358 variations in water transit time, or specific losses and/or inputs associated to the presence of the sewage network.

360 **3. Results**361 **3.1 Biogeochemical composition and typology of runoff-generating sources**

362 The median and range of concentrations of the biogeochemical parameters measured ~~for the runoff generating sources at the~~
 363 ~~sampling points~~ are reported in [Table A3](#) [Table A2](#) for major parameters, [Table A4](#) [Table A3](#) for metals, [Table A5](#) [Table A4](#)
 364 for the characteristics of DOM [and Table A6 for the microbial parameters, and Table A5 for microbial parameters](#). ~~These~~
 365 ~~concentrations~~[Concentrations](#) are illustrated in the form of a heatmap in [Figure 3](#)[Figure 3](#), coupled with a Hierarchical Cluster
 366 Analysis on the parameters and ~~the~~ sampling points.

367 The ~~biogeochemical compositions of~~ samples collected from the first forest sub-catchment (BOU) are all clustered together,
 368 ~~indicating similar concentrations marked by higher concentrations for Al and Cd, and higher values for S1 compared to the~~
 369 ~~other samples.~~ Samples collected from the second forest sub-catchment (VRY) ~~do not show clear clustering are also clustered~~
 370 ~~together but show a different pattern, marked by higher concentrations of SiO₂, showing a variable biogeochemical~~
 371 ~~composition, different from the BOU samples.~~ Samples collected at both grassland sub-catchments (VRN and REV) are well
 372 grouped, ~~showing similar compositions~~, despite their expected differences in terms of field capacity ([Figure 1](#)[Figure 1.B](#)).
 373 ~~They show high values for A1-254 and A2-254, indicating the presence of large organic matter molecules. Three~~ Three of the
 374 five samples collected from the agricultural sub-catchment (PNC) are clustered, ~~showing a similar composition~~, mostly
 375 characterised by higher concentrations of As [and](#), Co, Mn, Fe. ~~The other two PNC samples are not grouped with the other~~
 376 ~~three, indicating different compositions. Only one PNC sample is marked by high concentrations for the rum-2-bac DNA~~
 377 ~~marker.~~ Results show a ~~general good~~ clustering for ~~the five four~~ COR samples representing the colluvium aquifer, marked by
 378 significantly higher concentrations for a group of parameters including SiO₂, Li and Ba, in comparison to all other source
 379 samples. Among the five samples representing the colluvium aquifer (COR), two showed concentrations ~~of human marker~~
 380 ~~Bacteroides (HF183)~~ higher than 6 log₁₀ number of copies/100 mL ~~of human marker Bacteroides (HF183;~~ (see concentration
 381 range in [Table A6](#)[Table A4](#)), close to the SEW samples concentration, taken directly from wastewater (median 7 log₁₀ number
 382 of copies/100 mL). We considered that these samples were contaminated by wastewater, and removed them from the dataset.
 383 ~~Three of the five W wastewater samples (SEWRES) are also well clustered and, showing similar compositions, linked to a~~
 384 ~~large group of parameters comprised of major ions (e.g. Na⁺, K⁺PO₄³⁻), dissolved metals (e.g. Pb, Cu, Zn), DOC and DTN,~~
 385 ~~DOM indicators (A3-25⁴⁴ and SR) and microbial parameters (e.g. intI, HF183).~~ The urban and road runoff samples (PLR)
 386 show more variability as only ~~two three~~ of the four samples are grouped and marked by high concentrations of ~~NO₃⁻ and~~ V.



398 2). In contrast, we considered a single source associated to the presence of grassland, based on the clustering of the VRN and
399 REV samples. Each of the remaining sampling points was considered as a distinct source. Table 1 Table 4 shows the final
400 typology proposed to describe the runoff-generating sources; it and was used for the next step of our the present study,
401 including the new codes used to describe the nature of each source (AQU, FOR-1, FOR-2, GRA, AGR, AQU, SEW, URB and
402 SUR).

403

404 **Table 4** Typeology of the runoff-generating sources describing the nature of the sources that will be used for the creation of the
405 biogeochemical signatures and in the mixing model (source and colours codes are used thereafter in this study).

Sampling point	Source	Source code
BOU	Gneiss – Medium field capacity – Forest n°1	FOR-1
VRY	Gneiss – Medium field capacity – Forest n°2	FOR-2
VRN / REV	Gneiss – Low/Medium field capacity – Grassland	GRA
PNC	Gneiss – Medium field capacity – Agriculture	AGR
COR	Colluvium aquifer	AQU
RES	Sewer system	SEW
PLR	Urban and road surface runoff	URB
SUR	Quick surface runoff	SUR

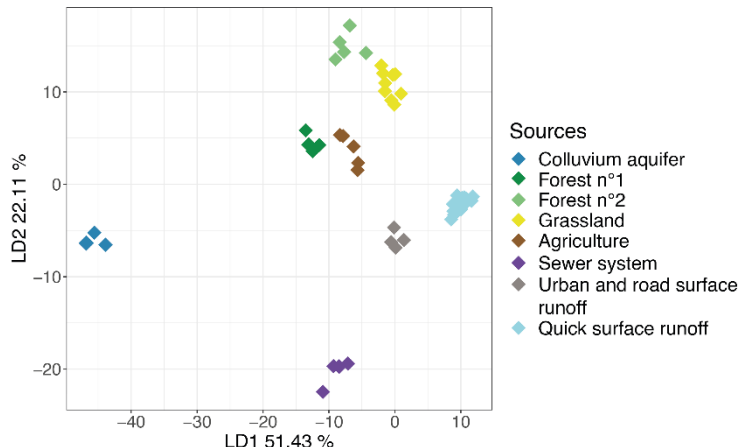
406

407 3.2 Building-up the biogeochemical signatures

408 After discarding the parameters considered to be non-additive and non-conservative according to their nature, 33 parameters
409 remained. Application of the range-test pointed out 13 other non-conservative parameters, with concentrations or values
410 outside the range observed for the source samples, mostly concerning the HPSEC indicators and the dissolved metals Al and
411 Co. The Kruskal-Wallis and Dunn tests showed two non-discriminant parameters: Ni and Ti with respective *p-values* of 0.06
412 and 0.93. Finally, the application of the LDA-Wilks lambda approach (Figure 4Figure 4) showed that an optimal selection of
413 15 tracers was sufficient to discriminate the 8eight sources. These tracers correspond to 7seven major parameters (Cl⁻, SO₄²⁻
414 , Ca²⁺, Na⁺, K⁺, Mg²⁺ and SiO₂), six6 dissolved metals (As, Ba, Cr, Li, Rb, Sr), and two DOM characteristics (DOC, spectral
415 slope S2). These parameters were used to build the biogeochemical signatures of each source. We, represented these
416 signaturesintheformofradarplots in Figure 5Figure 5.

417

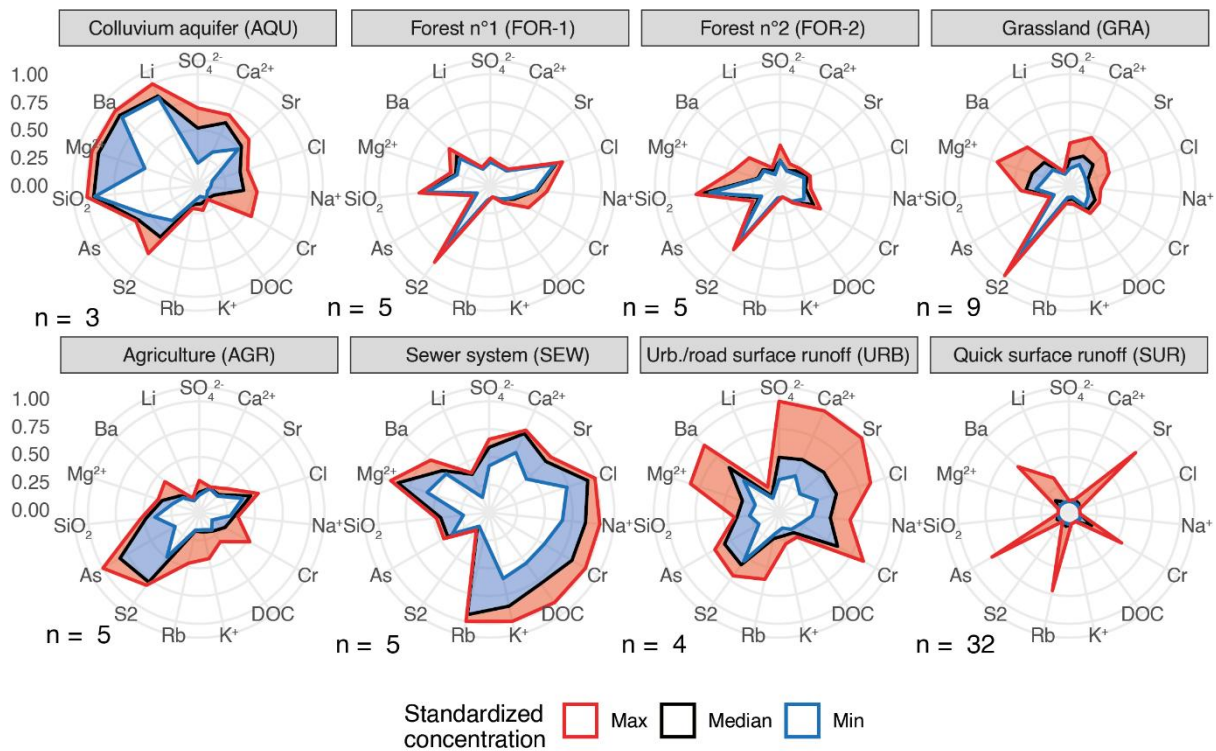
418



419

420 **Figure 4** – Source samples coloured according to the sources identified and projected along the axes created by the Linear
 421 Discriminant Analysis. The concentrations used correspond to the optimal selection of tracers resulting from the selection by
 422 minimisation of Wilks' lambda.

423



424

425 **Figure 5** – Biogeochemical signatures of the identified sources, in the form of a radar plot. The 15 tracers correspond to the optimal
 426 selection resulting from the reductionist approach. Maximum, median and minimum concentrations are presented after
 427 standardization across all 15 tracers. n: the number of samples per source; Urb: urban.

428

429 The FOR-1 and FOR-2 signatures show low and stable concentrations, with high values of the parameter S2, which is a spectral
430 slope calculated from absorption coefficients (350-400 nm), negatively correlated with the amount of aromatic carbon (Helms
431 et al., 2008). The GRA signature is even more marked by high values of S2. Headwater from forests and grasslands is thus
432 characterised by poorly aromatic DOM, which could be linked with high soil weathering (Y.H. Wang et al., 2023). Boukra et
433 al. (2023) showed similar results for surface waters from forest sub-catchments within the Ratier catchment, with a significant
434 difference between water from forest watershed, less aromatic and water from agricultural areas (vineyards), more aromatic.
435 Samples from the agricultural sub-catchment (AGR) also show higher values of the parameter S2, indicating low aromaticity,
436 but are also characterised by even higher concentrations of the trace element As. According to Liu et al. (2020), significant
437 concentrations of As can be observed in bovine manure, ranging from 2 to 17 mg/kg, which can explain the concentrations
438 obtained for the AGR samples (median of 4.25 µg/L). The AQU signature is particularly characterised by high values of SiO₂,
439 Mg²⁺, Ba and Li. Grandjouan et al. (2023) pointed out that this runoff generating source is mainly fed by a colluvium aquifer,
440 which significantly contributes to the Ratier stream volume outside of rainfall events, and attributed the high Li, Ba and Mg²⁺
441 concentrations to a geological origin. High SiO₂ concentrations are often observed in groundwater (Iorgulescu et al., 2005).
442 The URB signature shows variable concentrations, with wide ranges, for SO₄²⁻, Ca²⁺, Sr, Cr, Mg²⁺ and Ba. This composition
443 can be explained by the leaching of urban soils during rainy events, leading to the release of the elements that could have been
444 emitted by urban and road pollutions sources and deposited at the surface of these soils. This phenomenon can be amplified
445 by a first-flush effect, which favours the transport of elements for the first rains after long periods of dry weather (Deletic &
446 Orr, 2005). The SEW signature is marked by high concentrations for Cl⁻, Na⁺, Cr, DOC, K⁺, Rb and Mg²⁺, which is in line
447 with the classical composition of wastewater seen in the literature (e.g. Eme & Boutin, 2015; Fröhlich et al., 2008). The
448 variability observed for this source can be explained by the choice to collect the SEW samples during periods of rain (see
449 [Section- 2.2.1](#)). Therefore, water samples from the SEW source consist of a mix of wastewater, rainwater and road surface
450 runoff, since this is a combined sewer network. Finally, the signature obtained for SUR shows very low concentrations for
451 most of the 15 tracers, with the exception of high maximum concentrations for Sr, Cr, Rb, As, Ba. According to Becouze-
452 Lareure (2010), these high concentrations are associated with atmospheric inputs to rainwater from the industrial Rhône valley,
453 in the south-east of the Ratier catchment.

454 3.3 Hydrograph separation

455 3.3.1 Dry weather

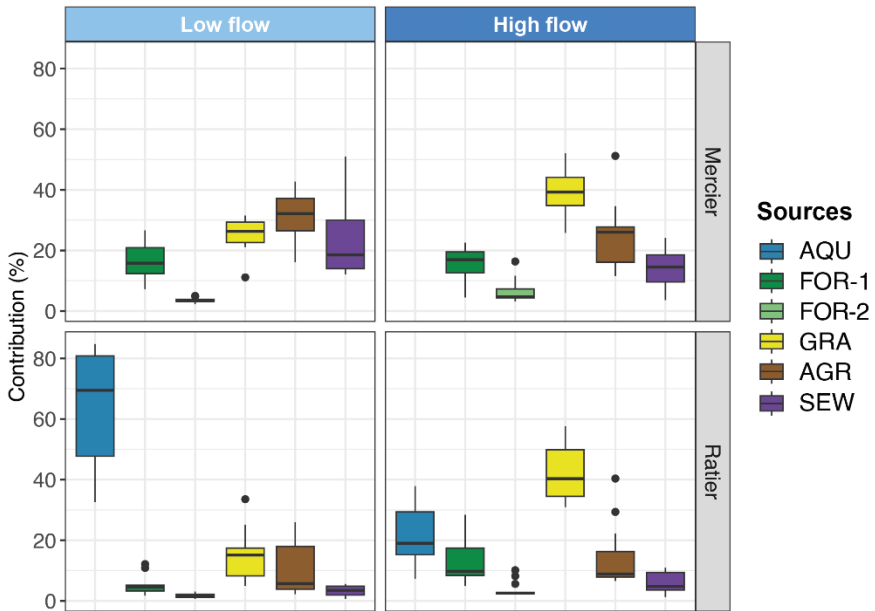
456 [Figure 6](#) shows the [results of the mixing model decomposition](#) relative contributions estimated for the 24 streamwater
457 samples collected at the Mercier and Ratier outlets outside from rainfall events. [Figure A1 represents the equivalent](#)
458 [contributions in daily volumes \(in m³\) that we calculated considering that the discharge measured at the time of sampling was](#)
459 [representative of the daily discharge](#). Results for the Mercier catchment showed little seasonality with similar results between
460 low and high flow. The AGR source contributed the most at low flow (up to 40% of total runoff) and the GRA source at high

461 flow (up to 50%). The SEW contribution was significant at both low and high flow conditions (between 10 and 50%), despite
462 the absence of sewer overflow devices within the Mercier catchment. The higher contributions at low flow suggest a continuous
463 input of wastewater that may originate from the sewer system itself to the Mercier streamwater. Wastewater from domestic
464 inputs or non-collective sanitation, not connected to the sewer system, could also contribute continuously to the Mercier
465 streamwater. We estimated median volume contributions of wastewater close to 30 m³/day at low flow and 800 m³/day at high
466 flow. As a comparison, Dubois et al. (2022) estimated the average daily wastewater flow from a French household around
467 0.311 m³/day, and Aussel et al. (2004) the wastewater discharge per inhabitants in France around 0.2 m³/day. Wastewater
468 contribution to the Mercier stream therefore represents the equivalent of a contribution of 100 households or 150 inhabitants.
469 (Dubois et al., 2022)(Aussel et al., 2004)Wastewater from domestic inputs or non-collective sanitation, not connected to the
470 sewer system, could also contribute continuously to the Mercier streamwater.

471
472 Results for the Ratier catchment show a significant influence of the AQU source with a high seasonality. Contribution of AQU
473 was predominant at low flow, up to 85% of total runoff (more than 500 m³/day). At high flow, although the estimated daily
474 volume for groundwater was higher than low flow (around 2 000 m³/day), the relative contribution was lower (around 20%).
475 It was; -from the colluvium aquifer was diluted by the other sources, such as and GRA, which showed a major relative
476 contribution (between 30 and 50%). The relative contributions estimated for SEW were lower than for the Mercier station
477 (below 10%), but the volume contribution remained stable (around 30 m³/day at low flow and 1 000 m³/day at high flow),
478 supporting the hypothesis of a constant wastewater transfer to streamwater, as seen for the Mercier catchment, which may be
479 diluted in the Ratier stream by the larger water flow.

480

481



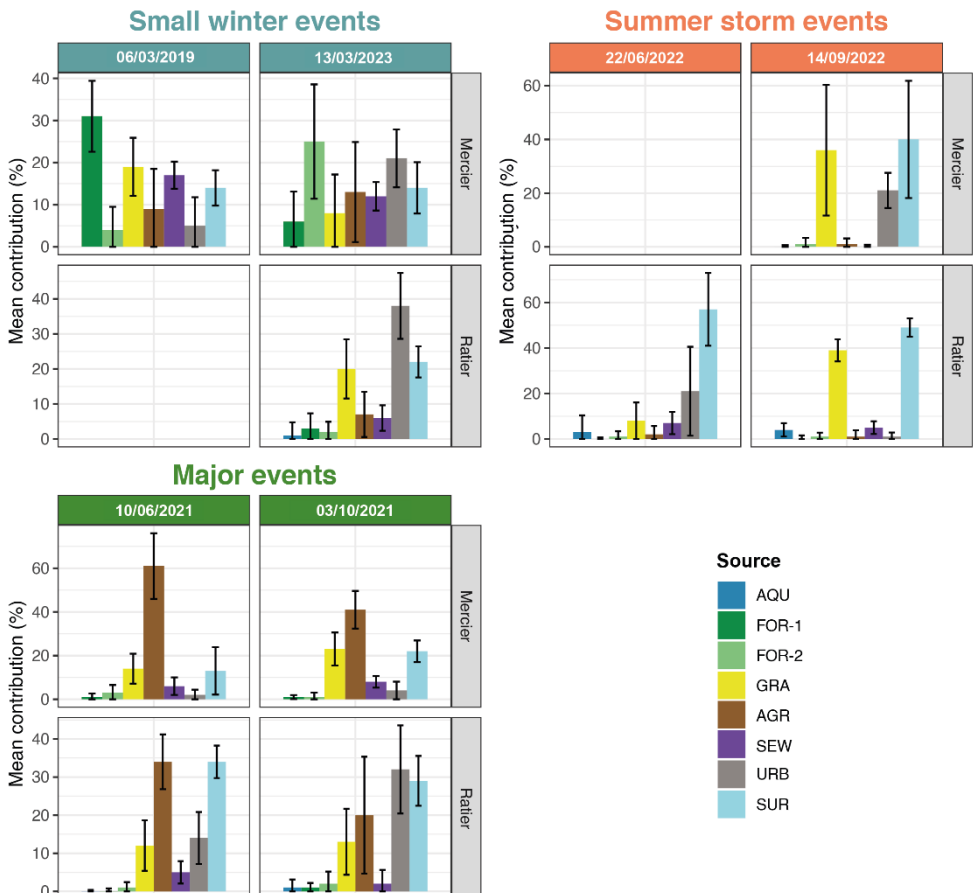
482

483 **Figure 6 – Sources contribution to runoff estimated for dry weather samples by the application of a biogeochemical decomposition**
 484 **using a Bayesian mixing model approach for the Mercier and Ratier catchments. Boxplots represent the median contribution,**
 485 **interquartile range (1st and 3rd quartiles), minimum and maximum values. Low flow samples correspond to a mean daily discharge**
 486 **lower than 20 L/s and high flow samples to a mean daily discharge higher than 20 L/s.**

487

488 3.3.2 Hydrological events: mean contributions

489 **Figure 7**
 490 **Figure 7** shows the mean of the source contributions estimated for each sampled hydrological event. **These means**
 491 **were**
 492 **We calculated these means**
 493 **calculated** from the individual results obtained by the application of the Bayesian mixing
 494 **model**
 495 **approach** on each streamwater sample (10 to 12 by event, see Section 2.2.2). **Figure 7**
 496 **Figure 7** also illustrates the uncertainty obtained for each event, in the form of the mean of the standard deviations obtained by applying each Bayesian
 mixing model decomposition, calculated from the sum of the squares of each deviation. **Further results**
will bear
presented
detailed below as the mean together with their associated uncertainty (noted as s.d. for standard deviation). Figure A2
 represents the contributions of each event in total volume, **which we**
calculated based on the relative contributions for each
 source and the total flow in m³.



497
498 **Figure 7 – Mean source contributions to the hydrological events sampled between March 2019 and March 2023 at the outlets of the**
499 **Mercier and Ratier catchments. The contributions correspond to the mean of the results obtained for each samples**
500 **decomposition** by the Bayesian mixing model ~~approach~~. The error bars correspond to the mean of the standard deviation calculated from the sum
501 **of the squares of the deviation. The events of 6 March 2019 at the Ratier station and 22 June 2022 at the Mercier station were not**
502 **collected.**

503

504 Results for small winter events show contrasted contributions. At the Mercier station, the major contribution was FOR-1 in
505 March 2019 (31%, *s.d. 8%*). ~~We calculated that the FOR-1 source was the major contribution in March 2023 (25%) but with~~
506 ~~relatively high uncertainty (s.d. 14%). In comparison, these contributions remained higher than those estimated at the Ratier station~~
507 ~~for both forest sources (5% in total, *s.d. 4%* and 4% *s.d. 3%*, respectively)~~, which is consistent with the results obtained ~~in dry weather~~. ~~The contributions of URB were significantly higher for the~~
508 ~~March 2023 event than for the March 2019 one, with 21% (*s.d. 7%*) at the Mercier station and 38% (*s.d. 9%*) at the Ratier~~
509 ~~station. This contrast can be explained by three times more rain in March 2023 (18 mm) than in March 2019 (7 mm). The~~
510 ~~source SEW showed high contributions at the Mercier station, similar to those estimated for dry weather (17 and 12%~~
511 ~~respectively for March 2023 and March 2019, and with calculated low uncertainty, (*s.d. 3%* for both events).~~

513 Results for the summer storm events showed predominant contributions of GRA, URB and SUR (>40%), but with relatively
514 higher uncertainties for the September 2022 event at the Mercier station (*s.d. 24%, 7% and 22%, respectively*) compared to
515 the Ratier station (*s.d. 5%, 2% and 4%, respectively*). The URB contribution for the September 2022 event was lower at the
516 Ratier (1%, *s.d. 1%*) than at the Mercier station (21%, *s.d. 7%*), ~~despite a higher urban spatial extent at the Mercier catchment,~~
517 ~~which can be explained by the greater presence of stormwater management structures for the Ratier than for the Mercier~~
518 ~~catchment. However, the contribution~~
519 ~~We calculated high contribution~~ of URB ~~was high~~ for the June 2022 event at the Ratier
520 station (21%), ~~which we but associated with~~ ~~high uncertainty (*s.d. 20%*)~~. ~~This result can be explained by the contribution~~
521 ~~from SEW (7%), which can be linked to sewer overflows. As these overflows are caused by excessive rainfall inputs in the~~
522 ~~sewer system, the volume transferred to streamwater during overflows is actually a mixture of wastewater, rainwater and urban~~
523 ~~surface water.~~

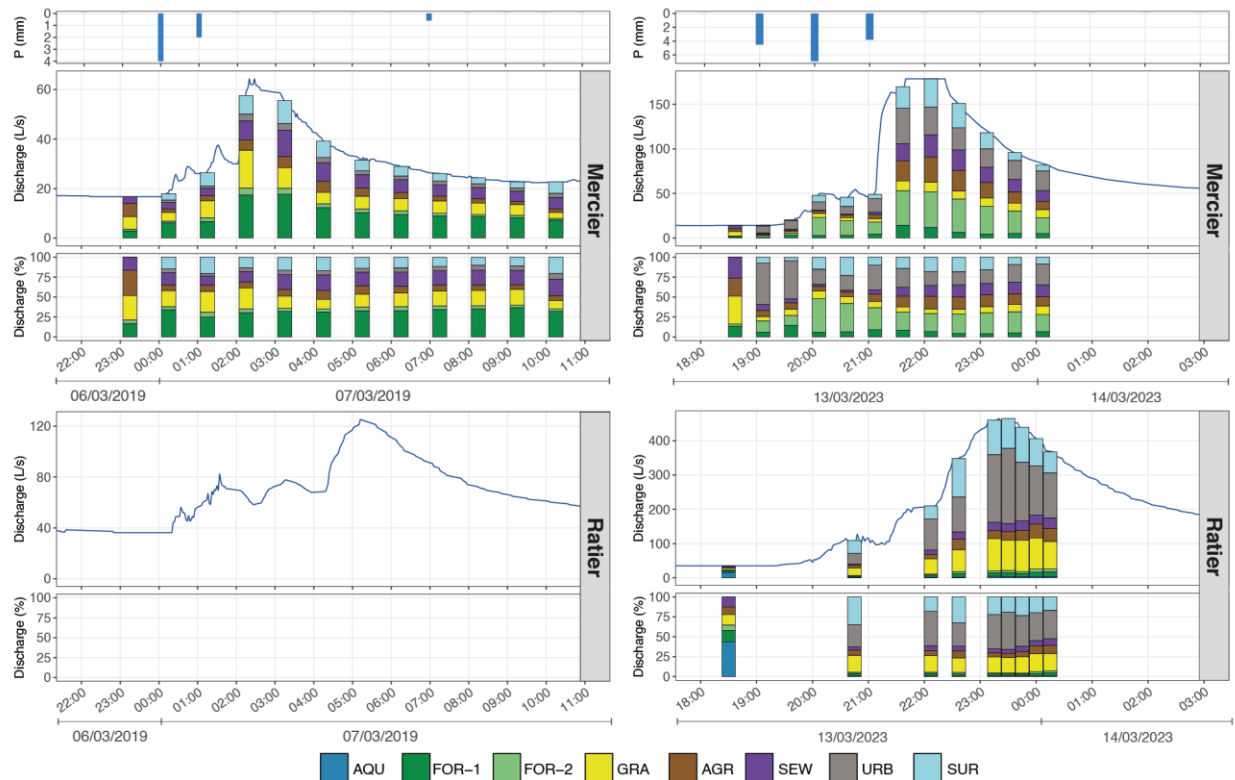
523 Results for both major events showed predominant contributions for AGR: 61% (*s.d. 15%*) and 41% (*s.d. 9%*) at the Mercier
524 station, 34% (*s.d. 7%*) and 20% (*s.d. 15%*) at the Ratier station. Uncertainty of the results were relatively low (<10%), with
525 the exception of the October 2021 event at the Ratier station (~~up to 20%~~). ~~The~~
526 ~~We calculated significant~~ SUR and URB contributions ~~were significant~~ at the Ratier ~~station~~ station, but with higher uncertainties for the urban source: 14% (*s.d. 7%*)
527 and 32% (*s.d. 12%*) for URB, 34% (*s.d. 4%*) and 29% (*s.d. 7%*) for SUR. ~~R~~
528 ~~Those estimated~~
529 ~~The SUR and URB contributions estimated~~ at the Mercier station were lower (~~<4% for URB and <22% for SUR~~), despite the high rainfall recorded for these
530 events (92 and 89 mm). ~~High SUR and URB contributions at the Ratier station can once again be explained by the sewer~~
531 ~~system overflows, spilling wastewater, rainwater and urban and road runoff water, which are less important in the Mercier~~
532 ~~catchment due to the absence of sewer overflow devices.~~ The relative contributions estimated for SEW ~~are were~~ low, but
533 showed high wastewater volumes when related to the total flow volume observed for each event. ~~By applying relative~~
534 ~~contributions to the observed discharge, we~~
535 ~~We estimated SEW contributions in terms of volume~~
536 ~~volume flows around~~ 900 and 2 000 m³ at the Mercier and Ratier stations, ~~respectively, during for~~ the May 2021 event, and around ~~960 and~~ 1 000 m³ for
537 ~~both stations during the October 2021 event (Figure A2). Such volumes of wastewater transferred to the stream are equivalent~~
538 ~~to the mean daily wastewater discharge for 3 000 to 6 500 French households, or for 5 000 to 10 000 inhabitants~~ (Aussel et al.,
539 2004; Dubois et al., 2022).

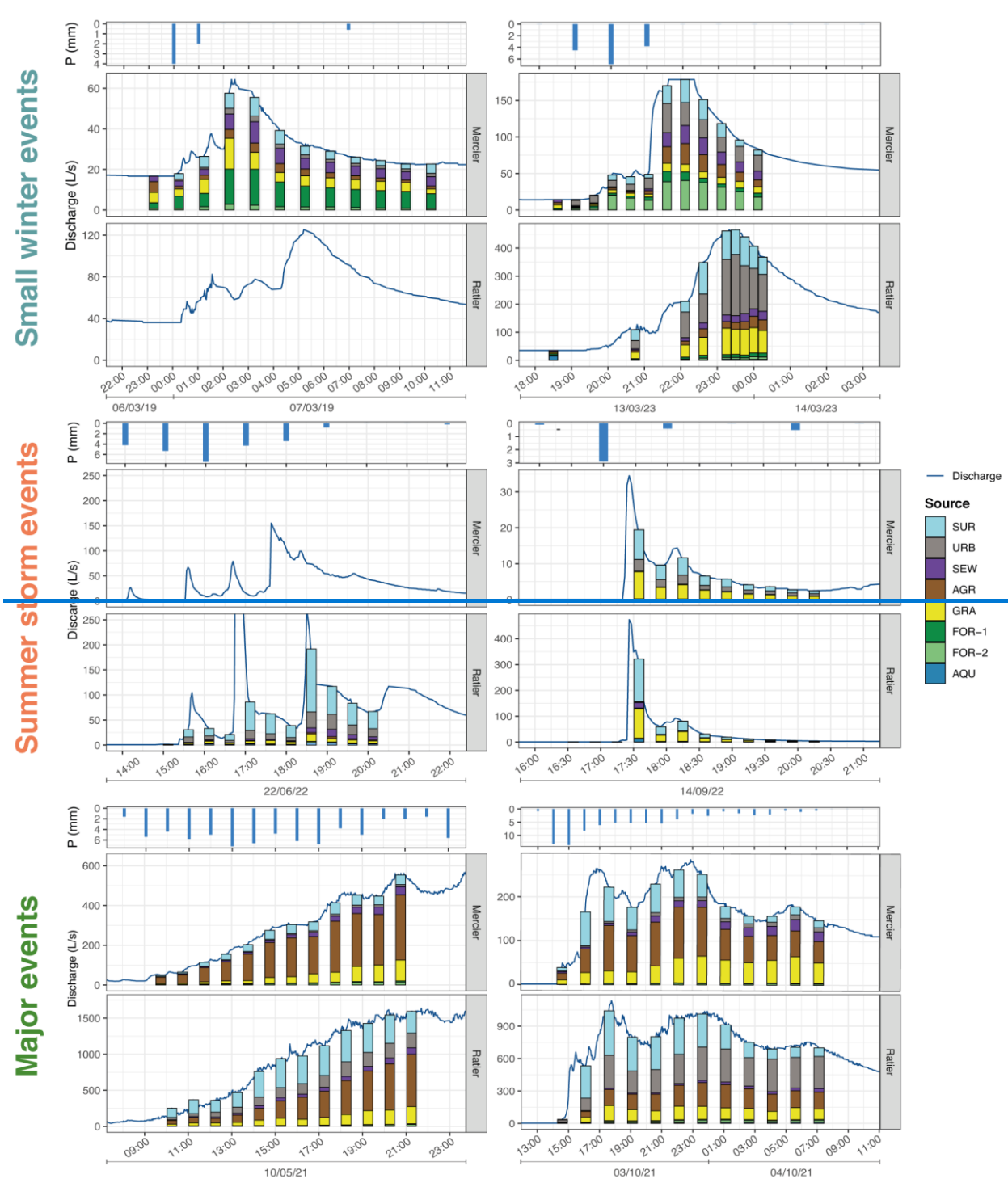
538 ~~The hydro meteorological conditions of the events appear to have a strong influence on the activated sources and their~~
539 ~~contributions. For the two small winter events, the contributions from grassland, agricultural areas, the sewer network and~~
540 ~~surface runoff are broadly consistent. However, there are significant differences in the contributions from urban and road~~
541 ~~runoff, which was higher in March 2023, and for those of the two forests between the March 2019 (FOR 1 as the main~~
542 ~~contribution) and the March 2023 events (FOR 2 as the main contribution). For summer storm events, the mean contributions~~
543 ~~estimated for both events are very consistent, with the exception of grassland and urban and road runoff. The major events~~
544 ~~showed the best consistency between the results for the Mercier and Ratier stations, despite some differences for sources linked~~
545 ~~to agriculture and urban road runoff. The spatial distribution of rainfall within the Ratier and Mercier catchments may also~~

546 help explain the differences observed between the two stations. Local rainfall variability may have influenced the activation
547 of specific sources, particularly those related to urban runoff and road surfaces.
548 The estimated results showed that similar sources have impacted the Mercier and Ratier catchments, with contributions
549 showing similar trends. However, mean contributions showed significant differences, which will require a more precise study
550 of the temporal variations over rain events.

551 **3.3.3 Hydrological events: temporal variability of contributions**

552 Figure 8Figure 8, Figure 9 and Erreur ! Source du renvoi introuvable. presents the results obtained by applying the
553 biogeochemical mixing model to the Mercier and Ratier streamwater samples decomposition results for the small winter events,
554 the summer storm events and the major events, respectively. They and It illustrates the temporal variability of the estimated
555 contributions for each source. The results are presented in the form of the figures of bars whose sizes correspond to the
556 instantaneous discharges associated to the decomposed samples. These results and the associated uncertainties are
557 detailed for each sampling time in Table A7, Table A8 and Table A9.





559

560 **Figure 8 – Precipitation and hydrograph separation results for the sampled events at the Mercier and Ratier stations for the small**
 561 **winter events of March 2021 and March 2023. The upper parts show bars whose sizes correspond to the instantaneous discharges**
 562 **(in L/s) associated to the decomposed samples. The lower parts show stacked the relative contributions in a range from 0 to 100%.**

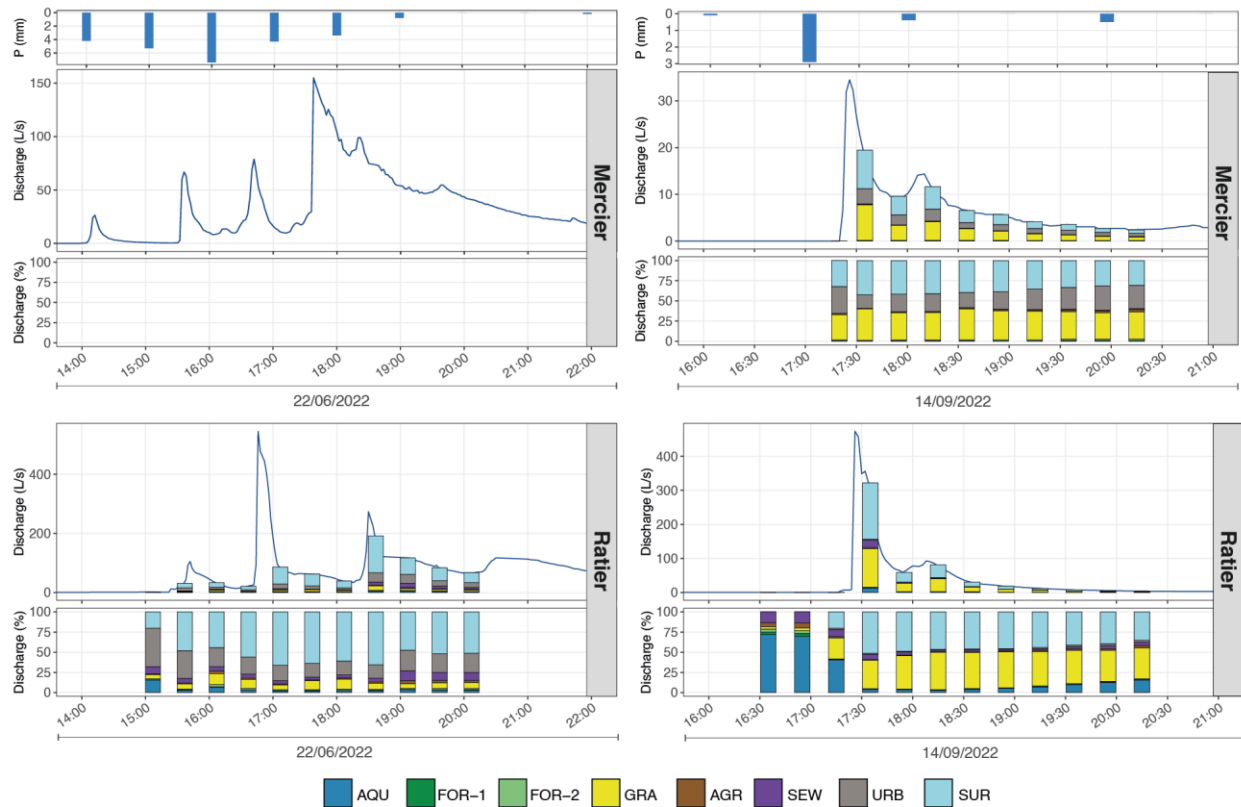
563 The results are shown according to the total outlet discharge (upper part) (below). The size of the bars corresponds to the
564 instantaneous discharge associated to each sample.

565

566

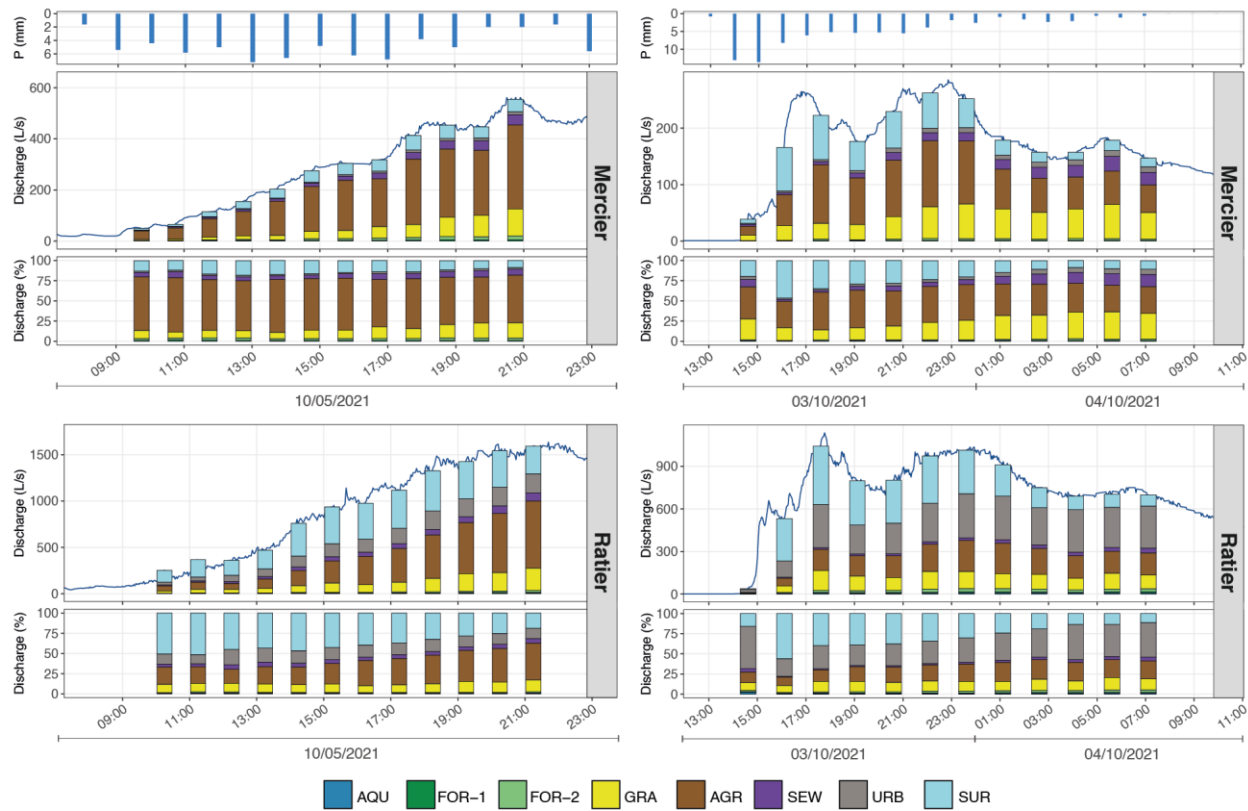
567 In the case of For the two small winter events of March 2019 and March 2023 (Figure 8), the first sample was taken before the
568 arrival of the rain. The contributions obtained for these samples prior to rainfall are consistent with the contributions
569 estimated for samples collected under dry weather conditions: the contribution of FOR-1 was around 15%, that of GRA around
570 30%, and that of AQU around 44% (s.d. 11%). However, results for FOR-1 and GRA are, however, associated with relatively
571 high uncertainties (s.d. 10 to 11% for FOR-1 and 1 to 23% for GRA). As for dry weather results, the contribution of SEW was
572 higher on the Mercier (up to 26%, s.d. 4 to 5%) than on the Ratier (13%, s.d. 7%). These results confirm the estimations
573 obtained for dry weather. These contributions changed once the rain started, but remained stable until the end for each small
574 winter event, despite the evolution of discharge. All these contributions estimated during rainfall are very close to the
575 mean contributions shown in Figure 7. The contribution of urban and road surface runoff in March 2023 for the Ratier
576 was the largest, right from the start of rainfall (52%, s.d. 7%), which might suggest particularly localized rainfall in urban
577 areas. The contribution of the sewer system remained stable over the March 2019 event for the Mercier, showing a rising input
578 of wastewater into the stream proportional to the total discharge. For the March 2023 event, the contribution of the sewer
579 system decreased during rainfall, suggesting a dilution of wastewater by rainwater in the sewer system.

580



581
 582 **Figure 9 – Precipitation and hydrograph separation results for the sampled events at the Mercier and Ratier stations for the summer**
 583 **storm events of June 2022 and September 2022. The upper parts show bars whose sizes correspond to the instantaneous discharges**
 584 **(in L/s) associated to the decomposed samples. The lower parts show stacked the relative contributions in a range from 0 to 100%.**

585
 586
 587 For the two summer storm events, most of the contributions remained relatively stable (Figure 9). The quick surface runoff
 588 (SUR) contributions remained the largest and the most variable ones. The estimated contributions for this source varied widely
 589 for the Ratier (from 20 to 65%), but were more stable for the Mercier (from 30 to 40%). However, uncertainties were relatively
 590 lower for the Ratier (s.d. between 9 and 23%), than for the Mercier (s.d. between 17 and 28%). The largest contributions for
 591 the Ratier were estimated during peak flows with relatively low uncertainty (max 65% for the Ratier for the June 2022 event,
 592 s.d. 15% and 50% for the September 2022 event, s.d. 4%). The estimated contributions from the sewer system (SEW) also
 593 varied along the events for the Ratier: from 3 to 12% (s.d. from 3 to 7%) in June 2022 and from 2 to 14% (s.d. from 1 to 6%)
 594 in September 2022. As with quick surface runoff, the largest contribution of wastewater was estimated for the peak flow for
 595 the Ratier (7% of total discharge). Such high contribution might be linked to the overflow of the sewer system, via the sewer
 596 overflow device or any other points of the sewer system.



597
 598 **Figure 10 – Precipitation and hydrograph separation results for the sampled events at the Mercier and Ratier stations for the major**
 599 **events of May 2021 and October 2021. The upper parts show bars whose sizes correspond to the instantaneous discharges (in L/s)**
 600 **associated to the decomposed samples. The lower parts show stacked the relative contributions in a range from 0 to 100%.**

601
 602
 603 Finally, the contributions estimated for the two major events also showed relatively low temporal variability (Figure 10). The
 604 predominant contribution was from agricultural areas (AGR), which varied from 3340 to 6066% for the Mercier (s.d. from 8
 605 to 17%), and from 2010 to 3045% for the Ratier. The AGR contributions at the Ratier showed higher uncertainties for the
 606 October 2021 event (s.d. from 9 to 20%) than for May 2021 event (s.d. 4 to 11%). The contribution of quick surface runoff
 607 showed higher variability, particularly for the event of October 2021, with a predominant part during the peak flow (475% for
 608 the Mercier, s.d. 6%, and 55% for the Ratier, s.d. 6%). For the May 2021 event, the quick surface runoff contribution never
 609 represented the majority, which can be explained by a less intense rainfall, favouring infiltration into the soil and the
 610 progressive rise of discharge. The contribution of wastewater was stable for the Ratier (around 5%, s.d. from 2 to 7%), but
 611 increased significantly for the Mercier (up to 15%, s.d. from 1 to 4%). These proportions represented contributions in volume
 612 up to 90 L/s at the Ratier for the May 2021 event, compared with the total discharge up to 1 500 L/s. In the case of this event,

613 the cumulative contribution could therefore represent volumes of wastewater transferred to the stream between 1 000 and 2 000
614 m³, equivalent to the mean daily wastewater discharge
615 of 4 000 inhabitants (Aussel et al., 2004).

616

617 4 Discussion

618 4.1 Questioning the representativeness and nature of the sources

619 The application of a mixing model for decomposition of streamflow implies that the sources are well represented by their
620 biogeochemical signatures. In our the present study, These signatures seem to have been were particularly well defined for
621 forests and grasslands. The signature of the colluvium aquifer (AQU) was more variable, but remained significantly marked
622 by high concentrations of Li, Ba and SiO₂ in all the samples. However, The concentrations of human-specific faecal markers
623 measured in several AQU samples confirm however, a contamination of the colluvium groundwater by wastewater. However,
624 The signatures for other sources showed much more variability (Figure 5Figure 5). Our The results question the
625 representativeness of these signatures and the initial assumptions on which the identification and sampling of these sources
626 were based.

627 Defining the biogeochemical signatures of agricultural sources based on a single sub-catchment turned out to be challenging
628 and highlighted three main difficulties. First, the catchment's characteristics made it difficult to delineate homogeneous sub-
629 catchments associated with specific agricultural activities (e.g. crop culture, bovine breeding). Second, observing even a small
630 flow at the outlets of agricultural sub-catchments was challenging due to the small size of these catchments and the
631 predominance of crops and grasslands, which are linked with lower field capacity. As a result, only one agricultural sub-
632 catchment could be identified and sampled. Third, the nature and intensity of agricultural activities can vary from one year to
633 the next, and even within a single year, leading to seasonal variations in the biogeochemical signatures. An example is the
634 absence of ruminant-specific bacterial faecal marker (rum-2-bac) in 4 out of 5 PNC samples. This questions the use of qPCR
635 as markers of source contributions, especially since microbial markers are strongly influenced by environmental factors like
636 water temperature (Marti et al., 2017). The use of more specific and persistent tracers, such as organic micropollutants, could
637 improve the identification and characterization of agricultural sources, in a more precise manner than the general tracers used
638 in this study, which were selected for their simplicity (Grandjouan et al., 2023). Previous studies have explored alternative
639 approaches. El Azzi et al. (2016) compared commonly used pesticides concentrations with results from a chemical mixing
640 model in an agricultural catchment. In doing so, they established a link between specific pesticides and vertical contributions
641 (surface runoff, subsurface runoff and groundwater). Banned pesticides that have not been used for several years could also
642 be used, as long-term storage often occurs in agricultural soils (Sandin et al., 2018). Our study could benefit from theseis
643 approach, specifying the contribution from the agricultural areas while taking into account and evaluating the vertical

644 contributions estimated by (Grandjouan et al., 2023) (i.e., saprolite flow, fractured gneiss flow and colluvium groundwater);
645 see Section 4.3). (Sandin et al., 2018)

646 We chose to sample water from the sewer system during rainfall events, in order to characterize the biogeochemical signature
647 of the water transferred to streamwater during overflows. However, our results show that the heterogeneous nature of these
648 watersamples, being a mixture of wastewater and urban and road surface runoff, has a strong influence on the contributions
649 estimated for the SEW and URB sources. The mixing model faces a first limitation as it is unable to distinguish wastewater
650 alone from urban and road surface runoff. Indeed, the SEW signature may have been diluted and influenced by the URB
651 signature, which already showed a variable biogeochemical composition. As a consequence, we may have overestimated the
652 SEW contributions during the events. Moreover, while Tran et al. (2019) investigated the presence of emerging contaminants,
653 including veterinary products, to characterise different sources such as agricultural stormwater runoff, but also encountered
654 high variability in concentrations.

655 For wastewater, our objective was to characterise the biogeochemical signature of the water discharged from the sewer system
656 by overflow. To achieve this, we sampled water from the sewer system during rainfall events. Given that the water sampled is
657 a mixture of wastewater and urban and road surface runoff, the obtained signature allowed us to estimate the contribution from
658 the sewer system during these events. However, the results for dry weather conditions may be less reliable, as only
659 wastewater is released through leaks in from the sewer system to the stream. Ideally, we should have built the wastewater
660 signature should have been built using samples collected from the sewer system under both dry weather and rainfall conditions,
661 to better distinguish the URB contributions from wastewater. The mixing model therefore faces a first limitation as it is unable
662 to distinguish wastewater alone from urban and road surface runoff.

663 Kuhlemann et al. (2021) estimated the contribution of wastewater in the Erpe peri-urban catchment (Germany) using an end
664 member mixing analysis, but also faced high uncertainties due to the similarities in concentrations between the composition
665 of wastewater and other runoff sources. The use of isotopic tracers (e.g. $\delta^{2}H$, $\delta^{18}O$) appears as a better way to estimate the
666 contribution of wastewater in a Bayesian mixing model (Marx et al., 2021).

667 In the case of urban and road runoff (URB), the first flush effect, implying the leaching of urban soils which favours high
668 concentrations of contaminants (e.g. Cu, Pb, Zn) after longer dry periods (Deletic & Orr, 2005), makes it difficult to
669 characterise a proper and unique signature. Indeed, (Simpson et al., 2023) characterised the runoff water quality from 13 urban
670 watersheds using classical tracers (i.e. nutrients, total suspended solids and heavy metals), but showed that the pollutant
671 concentration dependeds on the rainfall intensity, and that a first flush effect iswas not systematically observed. Innovative
672 tracers could help characterising this source, as forshowed by Lin et al. (2024) who used characteristics of DOMDOM
673 characteristics (with a fluorescence excitation-emission matrices spectroscopy technique) to estimate the contribution of road
674 runoff in an urban catchment. They found that the water generated by road runoff exhibited high aromaticity of DOM. In
675 ourthe present study, The values of the DOM parameter S2, which is negatively correlated with aromaticity, were indeed
676 lower for the URB signature than for the other sources. Hence, weOur results thus encourageconfirmed the usefulness of using
677 such DOM characteristics as tracers in a mixing model. In their study, Fröhlich et al. (2008) deduced the urban surface runoff

678 composition from the composition of streamwater during a peak flow, and from a Principal Component Analysis (PCA) as
679 described in Christophersen & Hooper (1992). They used a PCA prior to the application of a mixing model, which allowed to
680 confirm the correct number of sources and their biogeochemical composition.

681

682 Finally, as the quick surface runoff (SUR) composition was inferred from rainwater composition, it may be more or less distant
683 from reality. The hypothesis of a quick surface runoff keeping the biogeochemical signature of rainwater is questionable as
684 these waters can quickly accumulate elements (Langlois & Mehuis, 2003). Proper sampling of quick surface runoff should be
685 done in order to better estimate their contributions to streamwater, although such sampling can be difficult. Yet, Fröhlich et al.
686 (2008) conducted a similar study in the Dill Catchment (Germany), aimed at identifying runoff sources, including wastewater,
687 groundwater and stormwater flow, in which they regrouped surface and subsurface runoff. To do this, they sampled
688 streamwater from the outputs of sub-catchments characterized by specific geological formations, during baseflow and
689 hydrological events. They thus showed that the geochemical composition of stormflow was similar to the composition of
690 precipitation, showed in their study that the composition of stormflow headwaters was similar to precipitation, and
691 characterised by low-mineralization. Their results suggest the predominant contribution of low-mineralized waters for several
692 events, which support the use of the composition of rain to represent the quick surface runoff source, in cases where runoff
693 water could not be sampled. In any case, our study could benefit from a proper sampling of quick surface runoff in order to
694 better estimate their contributions to streamwater. Several studies analysed direct surface runoff water collected on soil surface
695 during hydrological events. Le et al. (2022) and Omogbehin & Oluwatimilehin (2022) both showed high concentrations of
696 DOC transferred from soils to the stream by overland flow. Omogbehin & Oluwatimilehin (2022) also showed low-
697 mineralised composition of the direct surface runoff water sampled. However, these two studies were conducted in a tropical
698 area, where direct surface runoff often occurs outside of urban areas. Such sampling appears to be difficult in temperate areas,
699 with less intensive rainfalls. (Omogbehin & Oluwatimilehin, 2022)

700 Another method to characterise sources is the use of stable isotopes (Le et al., 2022)(Wan et al., 2023)(Omogbehin &
701 Oluwatimilehin, 2022)(e.g. $\delta^2\text{H}$, $\delta^{18}\text{O}$). While many studies have used isotopic tracers in mixing models to estimate the
702 contributions from different runoff-generating sources, few of them were applied to peri-urban catchments with complex land
703 use distributions. Kuhlemann et al. (2021) estimated the contribution of wastewater in the Erpe peri-urban catchment
704 (Germany) using isotopic tracers together with physico-chemical parameters of water (i.e. conductivity and temperature of
705 water), in an Bayesian mixing model (using MixSIAR). However, they also faced high uncertainties due to the similarities in
706 concentrations between the composition of wastewater and other runoff sources. They concluded by recommending the use of
707 both isotopic and geochemical tracers to overcome these limitations.

708 4.2 Evaluating the estimated source contributions

709 The estimated contributions clearly invalidate the null hypothesis that source contributions are proportional to their spatial
710 extent (see Section 2.4). Spatial extent alone cannot explain the observed variability, and several additional factors appear to
711 influence source activation and the hydrological response of the catchments.

712 Contributions of the colluvium aquifer was constant, regardless of the hydro-meteorological conditions, as already shown by
713 Grandjouan et al. (2023).

714 The major contribution of forests to the Mercier stream during small winter events, and the fact that we sampled the two forest
715 sources at every campaign, independently from the hydro-meteorological conditions could be explained by the geological
716 characteristics of the upper part of the catchment. The saprolite horizon being thin in this area, it ~~is unable~~~~cannot~~~~to~~ store a
717 large volume of water. Alternatively, ~~t~~he constant flow generated by these springs may ~~thus~~ originate from the fractured
718 gneiss, fed by infiltrating rainwater. Recharge water can have a piston effect, pushing the groundwater retained within the
719 fractures towards the stream. Lachassagne et al. (2021) described a similar behaviour on another catchment characterised by
720 fractured crystalline formations and thin saprolite layer with (1) a vertical piston effect in the saprolite layer and (2) a
721 preferential deep horizontal flow in the fractures of the basement. During summer period, the minor forest's contribution can
722 be linked to the favoured retention of rainwater by the vegetation over runoff (Brujinzeel, 2004).

723 The variable contributions from grasslands and agricultural areas can be explained by the highly variable thickness of the
724 saprolite horizon downwards from forest - 1 to 20 m according to Goutaland (2009). The absence of runoff for the GRA and
725 AGR sources under low flow conditions in dry weather suggests the existence of throughs at the saprolite-gneiss interface in
726 which water can be stored and released discontinuously. This process was described as "fill-and-spill" by McDonnell et al.
727 (2021), and observed in the Panola catchment by Tromp-van Meerveld & McDonnell (2006), and in the Pocket lake catchment
728 by Spence & Woo (2003), both being characterised by a similar crystalline bedrock. They showed that the generation of
729 subsurface and surface flow in this context can be delayed, as it requires to meet sufficient rainfall amount to increase water
730 storage at the soil-bedrock boundary. When these conditions were not observed, Spence & Woo (2003) and Tromp-van
731 Meerveld & McDonnell (2006) noticed intermittent flow, which is similar to what we observed at the Mercier and Ratier
732 catchments. Indeed, contribution from agricultural lands are low or absent during summer storm events, and major during
733 major events, when rainfall amounts are sufficient. However, grasslands showed quicker and more frequent responses under
734 storm conditions. This difference may be linked to lower interception by vegetation, shallower root systems, and reduced water
735 demand in grasslands compared to forests or crops (Madani et al., 2017; Robinson & Dupeyrat, 2005).

736 Our results also show that summer storm events are often associated with generation of quick surface runoff. Indeed, ~~t~~Shi et
737 al., (2021) showed ~~indeed~~ that low antecedent soil moisture during summer periods can enhance the generation of quick surface
738 runoff. The lower general water demand from grassland may also favour the quick surface runoff for this particular land use.
739 As seen in Section 4.1, DOC can easily be transferred from soils to runoff water. As a consequence, the quick surface runoff
740 contribution generated on the surface of grasslands could have been considered as grassland contribution by the mixing model.

741 These results suggest that both vegetation type and antecedent soil moisture ~~jointly~~ influence the likelihood of quick surface
742 runoff generation.

743 (Grandjouan et al., 2023)(Grandjouan et al., 2023)(Grandjouan et al., 2023)The high contributions of SEW to the Mercier
744 streamwater suggest continuous wastewater inputs, either from sewer leakage or from non-collective sanitation. At the Ratier,
745 similar wastewater volumes ~~were~~ observed but diluted by larger baseflow. Grandjouan et al. (2023) already showed that the
746 sewer system has a strong influence on streamwater at dry weather, as they measured high concentrations for the HF183
747 human-specific faecal markers in both Mercier and Ratier streams (mean values of 2.4 and 2.5 \log_{10} copy nb/100mL,
748 respectively). Tran et al. (2019) observed a similar trend in agricultural areas with low residential and urban extent, with runoff
749 water composition similar to the composition of raw wastewater. They also suggest that these contributions come from leaks
750 from the sewer system. In ~~our~~the present study, during hydrological events, the increase in wastewater contributions can be
751 explained by sewer overflows, occurring both at the combined sewer overflow device and at other points of the network.
752 According to local sewer network managers, such overflows are frequent even during small winter events (<10 mm), due to
753 underside sewer infrastructure. Such wastewater transfer remains difficult to characterise in terms of both dynamics and
754 volume. Numerical modelling of the sewer leakage and overflow appears to be a promising way of quantifying these impacts
755 on groundwater (Nguyen et al., 2021).

756 Estimated contributions for urban and road runoff carry high uncertainty, partly because of the difficulty for the mixing model
757 ~~to~~ to distinguish wastewater from urban runoff (see Section 4.1), which may have influenced our calculations. Another factor
758 that could have influenced the URB contributions is ~~the~~ spatial rainfall variability, for example for the September 2022 event
759 where the Mercier showed higher URB contribution compared to the Ratier, despite being less urbanised. This phenomena is
760 particularly relevant during convective summer storm events, where precipitations are localised and lead to quick response of
761 urban areas, as showed by Kermadi et al. (2012) for the Yzeron catchment (which includes the Ratier catchment). The influence
762 of rainfall spatial distribution on hydrological response in urban areas is undergoing increasing study, especially through
763 hydrological modelling (Cristiano et al., 2017). Such studies encourage the use of high spatial resolution radar weather radar
764 images for studying rainfall spatial variability in small peri-urban catchments, although this remains uncommon (Emmanuel
765 et al., 2012).

766 (Grandjouan et al., 2023)Overall, these findings emphasize the role of the sewer system, rainfall spatial variability, water
767 pathways and transfer time in influencing source contributions, in addition to land use diversity.

768 **4.3 Improvement of the hydrological perceptual model of the Ratier and Mercier catchments**

769 (Grandjouan et al., 2023) ~~built a~~An initial perceptual hydrological model of the Ratier catchment, ~~describing~~ was built by
770 Grandjouan et al. (2023). This model ~~describes~~ the general hydrological behaviour of the catchment and the main contributions
771 to streamflow. ~~That model was based primarily on dry-weather observations; it allowed to~~ ~~and~~ identified three main sources
772 ~~including~~ The represented hydrological processes were deduced from catchment characteristics, field observations and a
773 mixing model applied on the basis of the biogeochemical quality of streamwater at the Mercier and Ratier outlets at dry weather

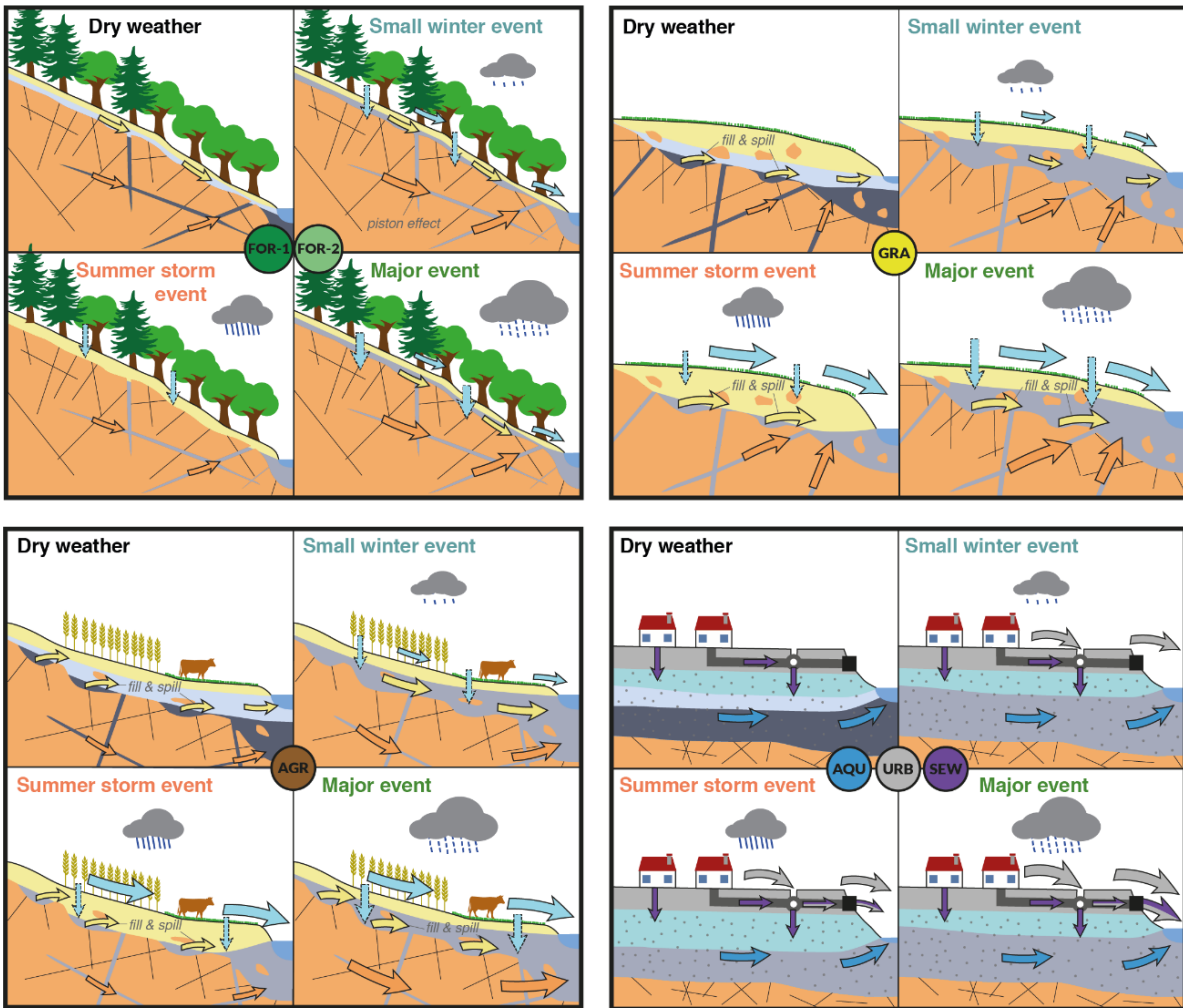
774 only. colluvium groundwater, fractured gneiss groundwater and the saprolite layer. The authors~~s~~ reported positive correlations
775 between discharge and saprolite contribution, and negative correlations between discharge and gneiss groundwater
776 contribution. However, they also showed unclear boundaries between both contributions, and suggested land use could play a
777 stronger role than geology in runoff generation. The extensive dataset obtained in the present study, including samples of
778 runoff generating sources, and the contributions estimated in our study, and together with the insights gained from results
779 presented in Sections 4.1 and 4.2, allows us to for the improvement of improve their initial representation of the catchment
780 hydrological behaviour by (Grandjouan et al., 2023) model, particularly in terms of hydrological behaviour at the hillslope
781 scale. (Grandjouan et al., 2023)

782 Figure 11Figure 9 illustrates the new hydrological perceptual model proposed for the Ratier and Mercier catchments. It
783 represents the hydrological dynamics of each identified source inferred from the contributions estimated during dry weather
784 and for different types of hydrological events that were consistently supported both by the results of the present study and
785 literature. We considered small winter events to occur at high flow, summer storm event at low flow, and major events either
786 at low or high flow.

787 In order to simplify the model, we chose to merge the two forest sources FOR-1 and FOR-2 as they represent similar areas of
788 the catchment. These sources are characterised by a shallow or absent saprolite depth, with the fractured gneiss formation
789 sometimes outcropping. The dominant process is groundwater contribution from fractured gneiss, recharged by rainfall and
790 mobilised through a piston effect. Contributions of forest is therefore considered stable in baseflow conditions, and higher
791 during small winter events. During summer storms, forest contributions remain minor due to strong canopy interception and
792 high evapotranspiration. For grasslands, generation of runoff is generally driven by a fill-and-spill mechanism within the
793 saprolite layer, producing intermittent sub-surface contributions. Hence, the contribution from grasslands therefore strongly
794 depends on the topography of the saprolite-gneiss boundary. Under storm conditions, grasslands also generate rapid surface
795 runoff due to low canopy interception and lower water demand. For agricultural lands, the same geological context suggests
796 fill-and-spill dynamics, but contributions diverge from grasslands because of higher crop water demand. Their role appears
797 minor in summer storms but can increase during major events. The sewer system contributes wastewater continuously through
798 leakage and sanitation losses. These contributions are especially marked in the Mercier catchment. Episodically during
799 hydrological events, it transfers a mixture of wastewater, urban and road surface runoff and rainwater is transferred to the
800 stream, through sewer overflows. The urban and road surface runoff contributions vary considerably as they strongly depends
801 on the urban area extent, on the presence of urban infrastructures that collects runoff water, and mostly on rainfall spatial
802 variability. Finally, the colluvium aquifer provides a nearly constant contribution regardless of hydrological conditions.
803 Evidence of wastewater contamination indicates that this source is characterised by both natural groundwater and
804 anthropogenic inputs.

805 This revised perceptual model show that runoff-generating sources are driven by both natural controls (geology, subsurface
806 storage, vegetation) and anthropogenic drivers (sewer leakage, urban runoff). The model confirms that land use and urban

807 elements (sewage system, impervious areas) exert a first-order control on hydrological responses. This new representation
808 provides a robust perceptual basis for future modelling and management of peri-urban catchments.
809
810
811



Urban elements

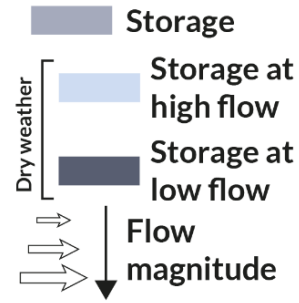
- Impervious surfaces
- Sewer system
- Sewer overflow device

Geology

- Colluvium
- Saprolite
- Fractured gneiss

Hydrology

- Infiltration
- Quick surface runoff
- Urban/road surface runoff
- Saprolite flow
- Sewage water
- Fractured gneiss groundwater flow
- Colluvium groundwater flow



812

813 Figure 119 – Improved perceptual model of the Ratier catchment, initially build by Grandjouan et al. (2023). Main contributions,
 814 estimated by the mixing model, are illustrated according to the nature of the sources and the four hydro-meteorological conditions
 815 studied, including dry weather, small winter event, summer storm event, major event. FOR-: forest; GRA-: grassland; AGR-:
 816 aquifer; URB-: urban and road surface runoff; SEW-: wastewater.

817 The two forest sources FOR 1 and FOR 2 were merged as they represent similar areas of the catchment. As their estimated
818 contributions were close, we assumed they have a similar hydrological behaviour. These sources are characterised by a shallow
819 or absent saprolite depth, with the fractured gneiss formation sometimes outcropping. The two forest sources were sampled
820 for every campaign, independently from the hydro meteorological conditions. As the saprolite horizon below the forest is
821 unable to store a large volume of water, the constant flow generated by these springs is expected to originate mainly from
822 fractures in the gneiss. These fractures are fed by infiltrating rainwater. Recharge water can have a piston effect, pushing the
823 groundwater retained within the fractures towards the stream. Lachassagne et al. (2021) described a similar behaviour on
824 another catchment characterised by fractured crystalline formations and thin saprolite layer (e.g. Alazard et al., 2016) with (1)
825 a vertical piston effect in the saprolite layer and (2) a preferential deep horizontal flow in the fractures of the basement. This
826 phenomenon could explain the major contribution of forests to the Mercier stream during small winter events. For summer
827 storm event, the forest's contribution is minor, as the retention of rainwater by the vegetation is favoured over runoff
828 (Bruijnzeel, 2004).

829 The runoff generated by grasslands could not be sampled under low flow conditions in dry weather. The highly variable
830 thickness of the saprolite horizon in this part of the catchment – 1 to 20 m according to Goutaland (2009) – suggests the
831 existence of throughs at the saprolite gneiss interface in which water can be stored and released discontinuously. This process
832 was described as “fill and spill” by (McDonnell et al., 2021) Tromp van Meerveld & McDonnell (2006), (Spence & Woo,
833 2003) for the Panola catchment, characterised by a similar crystalline geological formation. (Spence & Woo, 2003) (Tromp
834 van Meerveld & McDonnell, 2006) During summer storm events, the quick surface runoff is favoured in grasslands (Madani et
835 al., 2017; Robinson & Dupeyrat, 2005). The water demand is lower than in forested or cultivated areas (Madani et al., 2017).
836 Shi et al. (2021) showed that quick surface runoff is favoured with dry soils during summer periods.

837 Agricultural lands in the Ratier catchment are characterised by the same geological features as for grassland, and thus share
838 similar hydrological behaviour. The main difference was observed for the summer storm event, where the contributions of
839 agricultural lands were low compared to grasslands, which can be explained by the water demand of the crops culture. The
840 high contributions during major events are difficult to interpret, and could be due to local discontinuities, or the leaching of
841 agricultural soils containing agricultural specific tracers. But it is difficult to assess on the genericity of the results for
842 agricultural lands on the basis of a single sub catchment.

843 The contribution of the urban impacted colluvium aquifer was constant, regardless of the hydro meteorological conditions, as
844 already shown by Grandjouan et al. (2023). The concentrations of human specific fecal markers measured in several AQU
845 samples suggest a contamination of the colluvium groundwater by wastewater. Grandjouan et al. (2023) showed the significant
846 and constant input of wastewater into the soil and groundwater, through leaks in the sewer system or the use of septic tanks in
847 residential areas disconnected from the public network. This input is particularly significant in the Mercier catchment, where
848 wastewater represents a higher relative contribution than in the Ratier catchment when associated with their respective total
849 flow. (Tran et al., 2019) This wastewater contamination remains difficult to characterise in terms of both dynamics and volume.

850 Numerical modelling of the sewer leakage appears to be a promising way of quantifying these impacts on groundwater
851 (Nguyen et al., 2021).
852 (Kermadi et al., 2012)(Cristiano et al., 2017)(Emmanuel et al., 2012)

853 5 Conclusions

854 The objective of this study was to identify runoff-generating sources in a small peri-urban catchment, and estimate their
855 contributions to streamwater with a mixing model based on a biogeochemical dataset comprised of classical and original
856 tracers. This approach highlighted eight main sources linked to the spatial characteristics of the catchment: two types of forest
857 (FOR 1 and FOR 2), grassland (two sampled and merged as GRA), agricultural lands (AGR), a colluvium aquifer (AQU),
858 wastewater from the sewer system (SEW), urban and road surface runoff (URB) and quick surface runoff (SUR). A
859 comprehensive biogeochemical dataset was built to determine the signatures of these sources using a reductionist tracer
860 selection approach. Each signature included 15 tracers: seven major parameters (Cl^- , SO_4^{2-} , Ca^{2+} , Na^{2+} , K^+ , Mg^{2+}), six dissolved
861 metals (As, Ba, Cr, Li, Rb, Sr) and two characteristics of DOM (DOC, spectral slope S2). Results showed that the use of
862 indicators that are simple and cheap to analyse was sufficient to differentiate each source according to geological, pedological
863 and land use characteristics, or according to anthropogenic inputs.

864 The estimated source contributions were particularly stable in dry conditions, and significantly influenced by wastewater at
865 the Mercier catchment, and by the colluvium groundwater at the Ratier catchment. At the hydrological event scale, the source
866 contributions followed trends according to the hydro-meteorological state of the catchment: major contributions for forest,
867 grassland and agricultural sources during small winter events, predominant quick surface runoff contributions for summer
868 storm events, and major grassland and agricultural contributions for major events.

869 This approach showed the potential of the use of biogeochemical tracers to perform a spatial decomposition of water, based
870 on the physical characteristics of a catchment, in addition to a more traditional vertical decomposition. Results showed that
871 the use of indicators that are simple and cheap to analyse (major parameters, metals) together with more original tracers
872 (characteristics of DOM) was sufficient to differentiate each source according to geological, pedological and land use
873 characteristics, or according to anthropogenic inputs. This study also showed the need for precise accurate methods to identify
874 the runoff-generating sources and their biogeochemical signatures. An improvement of the approach would be a better
875 characterisation of the most variable sources, such as agricultural lands, urban and road surface runoff and sewer system
876 wastewater. Moreover, quick surface runoff needs to be collected and characterised to better estimate its contribution to
877 streamwater. The initial campaign plan aimed to sample this runoff at various locations representing forest, grassland and
878 agricultural areas. However, such sampling is challenging, as it requires being present at the right location and time due to the
879 ephemeral nature of surface runoff. The deployment of automatic samplers could help overcome these limitations and improve
880 data collection. Such sampling has already been implemented using a gutter-based collection system, as part of the ANR
881 CHYPSTER project, in the Claduègne catchment (Ardèche, France).

882 This study demonstrated the effectiveness of the proposed method in estimating the water pathways and the main contributions
883 within the studied catchments. The mixing model provided reliable estimates for several source contributions. Confidence in
884 the results was reinforced by the use of additional tracers beyond those used in the mixing model, such as DOM characteristics,
885 microbial parameters and other dissolved metals. The results obtained with the mixing model were consistent with the initial
886 perceptual hydrological model built for the Ratier catchment, and allowed us to build an improved version at the hillslope
887 scale. This new perceptual model provides a better understanding of the behaviour of these two nested catchments and their
888 hydrological dynamics depending on each hydro-meteorological condition.

889 More broadly, the application of mixing models in relation to land use remains relatively unexplored in the literature. This
890 study highlights the potential of such an approach when incorporating biogeochemical parameters and highlights the need for
891 further research in this direction.

892 This work illustrates the broader potential of mixing models to identified the spatial origin of streamflow and improve our
893 understanding of catchment hydrological behaviour. Such approaches could provide valuable insights for validating spatially
894 distributed hydrological models, which often face difficulties in adequately representing source contributions. More generally,
895 combining mixing models with land use and hydro-meteorological data may help to better anticipate the impacts of land
896 management or climate change on runoff-generation processes. Future research should therefore focus on integrating tracer-
897 based source characterisation with modelling frameworks, to improve both process representation and predictive capacity in
898 peri-urban catchments.

899

900

901

902 **Appendixes**

903 **Table A1 – Combinations obtained from the superimposition of factors describing sub-catchments (geology, field capacity, land use).**
 904 **The relative surface areas associated with each combination is provided for the Mercier and Ratier sub-catchments. Combinations**
 905 **with a relative area of less than 1% of the Ratier catchment are not detailed.**

<u>Geology</u>	<u>Field capacity</u>	<u>Land use</u>	<u>Agricultural activities</u>	<u>Surface (%)</u>	
				<u>Mercier</u>	<u>Ratier</u>
<u>Gneiss</u>	<u>Low</u>	<u>Forest</u>		<u>0</u>	<u>1</u>
		<u>Agriculture</u>	<u>Unspecified</u>	<u>0</u>	<u>3</u>
			<u>Bovine breeding</u>	<u>0</u>	<u>2</u>
		<u>Urban</u>		<u>0</u>	<u>5</u>
		<u>Forest</u>		<u>30</u>	<u>20</u>
	<u>Medium</u>		<u>Unspecified</u>	<u>20</u>	<u>6</u>
			<u>Permanent grassland</u>	<u>5</u>	<u>6</u>
		<u>Agriculture</u>	<u>Bovine breeding</u>	<u>0</u>	<u>3</u>
			<u>Cereal crop</u>	<u>2</u>	<u>5</u>
			<u>Equine breeding</u>	<u>0</u>	<u>1</u>
	<u>High</u>	<u>Urban</u>		<u>5</u>	<u>11</u>
		<u>Forest</u>		<u>0</u>	<u>4</u>
			<u>Unspecified</u>	<u>14</u>	<u>4</u>
			<u>Permanent grassland</u>	<u>1</u>	<u>3</u>
			<u>Bovine breeding</u>	<u>6</u>	<u>4</u>
			<u>Cereal crop</u>	<u>1</u>	<u>2</u>
		<u>Urban</u>		<u>0</u>	<u>2</u>
<u>Colluvium</u>	<u>Medium</u>	<u>Urban</u>		<u>0</u>	<u>3</u>

906

907

908 **Table A2 – Limits of quantification (LQ) and uncertainties (expanded U, k=2) for chemical parameters; they were calculated**
 909 **according to standard method NF-T90-210 (AFNOR, 2018) and NF ISO 11352 (AFNOR, 2013), respectively. For dissolved organic**
 910 **carbon (DOC), total dissolved nitrogen (NTD) and major ions, uncertainties were derived from results of interlaboratory tests. For**
 911 **trace elements, uncertainties were derived from regular analyses of Certified Reference Material TM-27-4 (lake water, Environment**
 912 **and Climate Change Canada).**

	Parameter	Unit	LQ	Uncertainty
Organic matter	DOC	mgC/L	0 ₋ 2	20%
	NTD	mgN/L	0 ₋ 2	20%
Major ions	Ca ²⁺	mg/L	4 ₋ 0	10%
	K ⁺	mg/L	1 ₋ 0	15%
	Mg ²⁺	mg/L	1 ₋ 0	13%
	Na ⁺	mg/L	1 ₋ 0	12%
	NH ₄ ⁺	mg/L	0 ₋ 02	14%
	Cl ⁻	mg/L	1 ₋ 0	7%
	NO ₂ ⁻	mg/L	0 ₋ 05	14%
	NO ₃ ⁻	mg/L	1 ₋ 0	13%
	PO ₄ ³⁻	mg/L	0 ₋ 1	14%
	SO ₄ ²⁻	mg/L	1 ₋ 00	9%
Trace elements	SiO ₂	mgSi/L	0 ₋ 5	12%
	Al	µg/L	2 ₋ 0	20%
	As	µg/L	0 ₋ 010	20%
	B	µg/L	2 ₋ 00	25%
	Ba	µg/L	0 ₋ 01	10%
	Cd	µg/L	0 ₋ 005	15%
	Co	µg/L	0 ₋ 005	15%
	Cr	µg/L	0 ₋ 02	20%
	Cu	µg/L	0 ₋ 05	15%
	Fe	µg/L	0 ₋ 10	15%
	Li	µg/L	0 ₋ 010	20%
	Mn	µg/L	0 ₋ 05	15%
	Mo	µg/L	0 ₋ 010	20%
	Ni	µg/L	0 ₋ 02	20%
	Pb	µg/L	0 ₋ 01	20%
	Rb	µg/L	0 ₋ 010	15%*
	Sr	µg/L	0 ₋ 05	10%
	Ti	µg/L	0 ₋ 05	25%
	U	µg/L	0 ₋ 005	20%
	V	µg/L	0 ₋ 005	20%
	Zn	µg/L	0 ₋ 50	25%

* uncertainty calculated using coefficient of variation of measured values only (no certified value for this element)

913
914

Table A3 – Summary of analytical results for major parameters in source samples. Values are concentrations in mg/L. All analytical results, quantification results and quality controls are available at: <https://entrepot.recherche.data.gouv.fr/dataVERSE/chypster/>

BOU (n=5)		VRY (n=5)		VRN (n=5)		REV (n=4)		PNC (n=5)		
Parameter	Median	Range								
<u>Ca²⁺</u>	11.1	10.5 - 12.3	6.2	5.5 - 13.0	22.7	21.1 - 40.4	14.6	12.1 - 18.6	15.7	15.3 - 16.9
<u>Cl⁻</u>	51.0	49.5 - 56.9	16.0	13.2 - 18.6	6.63	5.8 - 26.7	9.7	7.0 - 16.7	38.0	30.7 - 44.8
<u>K⁺</u>	1.0	1.0 - 1.0	1.0	1.0 - 1.0	1.6	1.5 - 2.6	1.0	1.0 - 1.0	2.7	2.2 - 8.3
<u>Mg²⁺</u>	2.8	2.7 - 3.2	1.9	1.8 - 3.7	3.2	3.0 - 5.7	2.4	2.0 - 3.1	3.0	2.2 - 3.3
<u>Na⁺</u>	26.8	25.7 - 34.2	11.3	10.2 - 15.3	8.6	8.19 - 15.4	6.3	5.6 - 7.8	18.6	15.6 - 21.1
<u>SiO₂</u>	20.4	18.4 - 21.1	24.1	20.8 - 25.6	12.7	10.7 - 13.5	11.1	8.3 - 11.9	14.9	11.9 - 16.8
<u>SO₄²⁻</u>	13.8	12.2 - 15.9	14.1	13.6 - 28.0	18.7	14.9 - 30.0	9.3	6.6 - 13.4	9.5	6.8 - 20.4
COR (n=5)		PLR (n=4)		RES (n=5)						
Parameter	Median	Range	Median	Range	Median	Range				
<u>Ca²⁺</u>	55.8	25.3 - 64	45.4	28.6 - 96.3	72.8	52.9 - 76.2				
<u>Cl⁻</u>	29.9	4.6 - 45.7	43.4	25.9 - 74.4	80.8	61.9 - 87.4				
<u>K⁺</u>	2.9	0.9 - 3.8	3.5	1.9 - 5.2	18.3	12.5 - 21.5				
<u>Mg²⁺</u>	7.5	4.2 - 8.2	3.0	2.0 - 6.9	7.1	4.9 - 7.6				
<u>Na⁺</u>	26.5	2.3 - 37.0	30.3	17.0 - 44.7	63.2	46.4 - 73.6				
<u>SiO₂</u>	32.0	15.5 - 34.8	11.1	6.8 - 12.0	13.3	5.5 - 14.8				
<u>SO₄²⁻</u>	43.7	11.4 - 62.2	41.6	21.1 - 93.2	50.8	33.8 - 58.3				

Table A4 – Summary of analytical results for dissolved metals in source samples. Values are concentrations in ug/L. All analytical results, quantification results and quality controls are available at: <https://entrepot.recherche.data.gouv.fr/dataVERSE/chypster/>

BOU (n=5)			VRY (n=5)		VRN (n=5)		REV (n=4)		PNC (n=5)	
Parameter	Median	Range	Median	Range	Median	Range	Median	Range	Median	Range
Al	126	82.8 - 142	62.5	45.3 - 105	43.2	8.40 - 70.5	75.1	24.3 - 102	29.2	18.9 - 55.9
As	0.49	0.25 - 0.52	0.73	0.58 - 1.11	0.63	0.43 - 0.68	0.53	0.45 - 0.66	4.25	0.93 - 5.28
B	3.00	2.80 - 4.70	3.90	3.70 - 5.00	11.4	8.30 - 18.6	2.80	2.20 - 4.20	2.60	0.20 - 7.30
Ba	20.0	17.9 - 24.4	10.4	9.70 - 18.4	15.4	13.3 - 25.4	13.4	10.4 - 18.7	11.2	9.73 - 20.5
Cd	0.073	0.064 - 0.096	0.023	0.010 - 0.030	0.008	0.005 - 0.021	0.020	0.012 - 0.027	0.009	0.005 - 0.024
Co	0.160	0.144 - 0.173	0.109	0.063 - 0.320	0.125	0.112 - 0.135	0.139	0.115 - 0.213	0.779	0.079 - 1.28
Cr	0.23	0.20 - 0.43	0.37	0.23 - 0.46	0.19	0.15 - 0.29	0.30	0.24 - 0.31	0.26	0.08 - 0.61
Cu	0.42	0.10 - 0.67	0.66	0.10 - 2.75	3.70	3.23 - 4.23	1.77	0.77 - 2.89	0.94	0.74 - 11.3
Fe	24.4	9.10 - 34.1	46.6	13.1 - 106	30.3	5.79 - 59.6	35.3	16.9 - 48.8	285	13.4 - 897
Li	1.84	1.75 - 2.27	1.42	0.29 - 2.15	0.692	0.622 - 0.753	0.756	0.391 - 1.08	0.759	0.483 - 1.23
Mn	41.7	9.15 - 12.2	12.6	4.84 - 34.6	1.17	0.66 - 4.03	3.86	1.16 - 8.52	556	1.17 - 1209
Mo	0.045	0.029 - 0.058	0.048	0.029 - 0.057	0.158	0.108 - 0.185	0.0305	0.010 - 0.037	0.304	0.067 - 0.488
Ni	1.13	1.09 - 1.66	1.42	1.14 - 1.67	1.35	0.99 - 2.80	0.99	0.85 - 1.61	0.88	0.44 - 1.08
Pb	0.019	0.005 - 0.032	0.130	0.082 - 0.146	0.013	0.005 - 0.094	0.014	0.005 - 0.024	0.060	0.005 - 0.312
Rb	0.850	0.719 - 1.21	0.724	0.327 - 1.06	0.716	0.598 - 1.19	0.396	0.209 - 0.471	1.30	1.13 - 6.53
Sr	44.1	41.4 - 51.3	40.5	26.5 - 56.0	81.4	75.5 - 138	46.8	27.0 - 68.2	58.9	51.7 - 94.4
Ti	0.52	0.05 - 1.29	1.26	0.27 - 3.94	0.90	0.18 - 2.14	1.80	0.58 - 2.68	0.86	0.75 - 2.73
U	0.298	0.211 - 0.349	0.157	0.005 - 0.303	0.244	0.117 - 0.316	0.148	0.033 - 0.257	0.120	0.079 - 1.00
V	0.289	0.213 - 0.357	0.331	0.229 - 0.403	0.308	0.276 - 0.344	0.297	0.276 - 0.683	0.381	0.258 - 1.02
Zn	1.74	1.33 - 2.16	1.57	0.10 - 1.85	2.63	1.79 - 6.81	2.18	0.93 - 2.76	1.95	1.30 - 73.4
COR (n=5)			PLR (n=4)		RES (n=5)					
Parameter	Median	Range	Median	Range	Median	Range				
Al	13.8	7.99 - 97.9	54.3	15.5 - 62.7	17.1	13.9 - 47.5				
As	3.05	1.99 - 3.47	2.75	0.68 - 3.34	1.97	1.68 - 2.20				
B	17.7	14.9 - 46.5	31.4	15.6 - 36.4	47.9	21.3 - 89.6				
Ba	46.4	28.8 - 49.2	29.7	21.0 - 44.5	27.8	25.6 - 34.7				
Cd	0.008	0.005 - 0.013	0.027	0.014 - 0.058	0.021	0.014 - 0.107				
Co	0.116	0.066 - 0.137	0.276	0.145 - 0.482	0.503	0.122 - 0.579				
Cr	0.226	0.033 - 0.65	0.72	0.19 - 1.08	1.06	0.67 - 1.25				
Cu	2.00	0.10 - 3.66	8.57	1.07 - 14.3	19.6	9.98 - 24.8				
Fe	64.1	37.1 - 99.5	22.8	8.00 - 62.3	50.4	27.9 - 104				
Li	21.1	9.93 - 24.9	1.79	1.15 - 4.22	7.68	1.40 - 8.08				
Mn	33.2	17.8 - 81.6	13.8	0.69 - 59.7	28.9	3.91 - 54.4				
Mo	0.901	0.747 - 1.19	1.20	0.05 - 1.57	1.06	0.749 - 1.39				
Ni	0.509	0.020 - 0.594	0.960	0.580 - 1.19	1.56	0.560 - 2.15				
Pb	0.124	0.049 - 0.202	0.142	0.039 - 0.588	0.460	0.322 - 0.528				
Rb	1.55	0.831 - 2.00	2.53	1.81 - 9.15	14.9	2.22 - 16.0				
Sr	181	126 - 219	186	64.1 - 379	247	148 - 272				
Ti	0.236	0.126 - 5.67	0.48	0.320 - 3.07	1.45	0.520 - 2.13				
U	0.558	0.544 - 0.906	1.69	0.100 - 2.80	1.29	1.12 - 2.73				
V	0.919	0.561 - 0.985	1.51	0.408 - 3.53	0.598	0.272 - 1.30				
Zn	13.6	4.3 - 13.7	18.6	4.56 - 48.6	36.6	20.4 - 44.2				

Table A5 – Summary of analytical results for characteristics of dissolved organic matter in source samples. All analytical results, quantification results and quality controls are available at: <https://entrepot.recherche.data.gouv.fr/dataverse/chypster/>

BOU (n=5)			VRY (n=5)		VRN (n=5)		REV (n=4)		PNC (n=5)			
Parameter	Unit	Median	Range									
DOC	mg/L	2.9	2.7 - 4.6	4.2	3.8 - 4.7	7.5	6.2 - 8.2	8.4	8.4 - 10.1	5.3	4.6 - 10.8	
E2:E3	-	7.4	6.8 - 7.7	6.4	6.1 - 6.6	6.7	6.3 - 6.9	6.9	6.4 - 7.3	4.7	4.5 - 6.3	
E2:E4	-	24.9	21.2 - 28.9	20.6	19.2 - 21.8	25.2	22.8 - 26.5	27.7	24.0 - 29.6	17.7	13.5 - 21.5	
E3:E4	-	6.9	6.2 - 7.1	5.9	5.7 - 6.1	6.7	6.3 - 7.0	7.1	6.5 - 7.6	5.3	4.5 - 6.4	
E4:E6	-	8.8	3.5 - 12.8	10.2	7.2 - 17.4	11.2	6.4 - 30.3	9.1	6.0 - 12.4	11.6	5.9 - 21.1	
SUVA	L/mgC/m	2.2	2.1 - 2.4	2.7	2.5 - 3.0	2.9	2.6 - 3.0	2.8	2.6 - 3.0	3.1	2.9 - 4.3	
S1	nm ⁻¹	0.0160	0.0158 - 0.0163	0.0156	0.0153 - 0.0158	0.0153	0.0151 - 0.0155	0.0151	0.0150 - 0.0155	0.0134	0.0119 - 0.0144	
S2	nm ⁻¹ nm ⁻¹	0.0196	0.0184 - 0.0203	0.0185	0.0183 - 0.0187	0.0205	0.0199 - 0.0209	0.0213	0.0207 - 0.0220	0.0194	0.0162 - 0.0198	
SR	-	0.83	0.79 - 0.86	0.84	0.83 - 0.86	0.76	0.72 - 0.77	0.71	0.70 - 0.73	0.71	0.60 - 0.83	
Mn-254	Da	417	323 - 460	542	394 - 593	616	548 - 695	607	596 - 636	569	526 - 703	
Mw-254	Da	1718	1352 - 2365	1644	1049 - 2364	1543	1146 - 1766	1266	1188 - 1649	1423	1198 - 1858	
disp-254	-	4.19	3.02 - 7.04	2.77	2.52 - 5.13	2.42	1.86 - 2.96	2.05	1.93 - 2.77	2.31	2.02 - 3.28	
A0-254	-	4552	2486 - 7349	4772	2165 - 8337	4627	407 - 10478	2404	1501 - 7710	2265	1209 - 4962	
A1-254	-	21850	15215 - 34702	47737	46348 - 59736	117263	86123 - 138631	110027	104294 - 117502	67331	50782 - 114518	
A2-254	-	48675	38354 - 83965	78227	70245 - 93519	188721	146038 - 204308	216676.5	185118 - 228952	121649	80952 - 176082	
A3-254	-	54560	47984 - 128755	65957	54730 - 85950	96041	77790 - 123959	112563	102393 - 121161	62096	53834 - 112852	
COR (n=5)			PLR (n=4)		RES (n=5)							
Parameter	Unit	Median	Range	Median	Range	Median	Range					
DOC	mg/L	3.5	2.0 - 10.1	6.1	4.4 - 8.4	32.7	22.1 - 42.6					
E2:E3	-	5.2	4.8 - 6.9	5.9	5.8 - 6.1	5.4	4.9 - 7.6					
E2:E4	-	14.9	11.9 - 23.3	18.9	17.2 - 20.6	11.3	10.5 - 14.9					
E3:E4	-	5.0	4.6 - 7.1	5.5	5.3 - 5.9	4.3	3.9 - 5.7					
E4:E6	-	5.6	3.0 - 15.1	9.1	7.8 - 10.5	6.8	5.9 - 8.7					
SUVA	L/mgC/m	2.0	0.8 - 2.6	2.8	2.4 - 3.0	1.3	0.9 - 1.4					
S1	nm ⁻¹ nm ⁻¹	0.0123	0.0118 - 0.0145	0.0144	0.0144 - 0.0153	0.0161	0.0104 - 0.0168					
S2	nm ⁻¹ nm ⁻¹	0.0163	0.0150 - 0.0192	0.0172	0.0167 - 0.0186	0.0127	0.0123 - 0.0128					
SR	-	0.80	0.64 - 0.85	0.84	0.77 - 0.92	1.28	0.82 - 1.33					
Mn-254	Da	451	434 - 670	727	621 - 885	424	383 - 579					
Mw-254	Da	2031	941 - 2432	1765	1571 - 1974	1390	1204 - 2201					
disp-254	-	3.03	2.17 - 5.39	2.21	2.00 - 3.18	3.14	2.88 - 4.00					
A0-254	-	4797	144 - 7402	3085	2560 - 9811	6713	4296 - 14343					
A1-254	-	33782	18214 - 53643	128469	65410 - 156480	73927	61653 - 100544					
A2-254	-	45994	20069 - 65362	137524	86234 - 207418	116338	93322 - 171777					
A3-254	-	43102	16900 - 55750	54241	35715 - 114897	129258	85384 - 218065					

Table A6 – Summary of analytical results for microbial parameters in source samples. Values are concentrations in log10 number of copies/100 mL.

BOU (n=5)			VRY (n=5)		VRN (n=5)		REV (n=4)		PNC (n=5)				
Parameter	Median	Range	Median	Range	Median	Range	Median	Range	Median	Range			
G16S	7.3	7.0 – 7.5	7.8	7.4 – 9.1	7.8	7.8 – 8.6	8.8	8.8 – 8.9	8.4	7.2 – 9.4			
B7T	3.7	2.6 – 4.2	4.0	0.0 – 5.1	5.0	0.0 – 5.5	6.3	0.0 – 6.7	6.2	5.1 – 6.7			
HF183	0.0	0.0 – 0.0	0.0	0.0 – 0.0	0.0	0.0 – 1.9	0.0	0.0 – 0.0	0.0	0.0 – 0.0			
rum-2-bac	0.0	0.0 – 0.0	0.0	0.0 – 0.0	0.0	0.0 – 0.0	0.0	0.0 – 0.0	0.0	0.0 – 6.0			
B7S	0.0	0.0 – 3.5	0.0	0.0 – 0.0	0.0	0.0 – 2.2	0.0	0.0 – 0.0	0.0	0.0 – 3.0			
int1	0.0	0.0 – 4.1	0.0	0.0 – 3.9	0.0	0.0 – 4.8	3.3	0.0 – 3.4	0.0	0.0 – 0.0			
int2	0.0	0.0 – 3.8	0.0	0.0 – 0.0	0.0	0.0 – 0.0	0.0	0.0 – 0.0	1.4	0.0 – 3.4			
COR (n=5)			PLR (n=4)		RES (n=5)								
Parameter	Median	Range	Median	Range	Median	Range							
G16S	9.4	8.6 – 9.6	9.4	9.2 – 9.5	10.4	9.5 – 11.4							
B7T	6.3	6.2 – 7.3	6.5	6.5 – 6.6	8.80	7.9 – 9.6							
HF183	3.7	3.5 – 6.3	3.5	3.1 – 3.6	7.05	5.7 – 7.5							
rum-2-bac	0.0	0.0 – 0.0	0.0	0.0 – 0.0	4.15	3.4 – 4.6							
B7S	3.6	3.3 – 4.6	5.1	5.0 – 6.2	7.05	6.6 – 7.9							
int1	0.0	0.0 – 3.0	4.0	0.0 – 4.5	5.25	4.3 – 6.0							
int2	4.4	0.0 – 6.0	2.8	0.0 – 3.4	6.30	5.0 – 6.5							

Table A7 – Mean contributions and standard deviations of estimations obtained for the decomposition of streamwater samples collected during small winter events in March 2019 and March 2023. The values correspond to the relative parts of flow for each time step as a percentage.

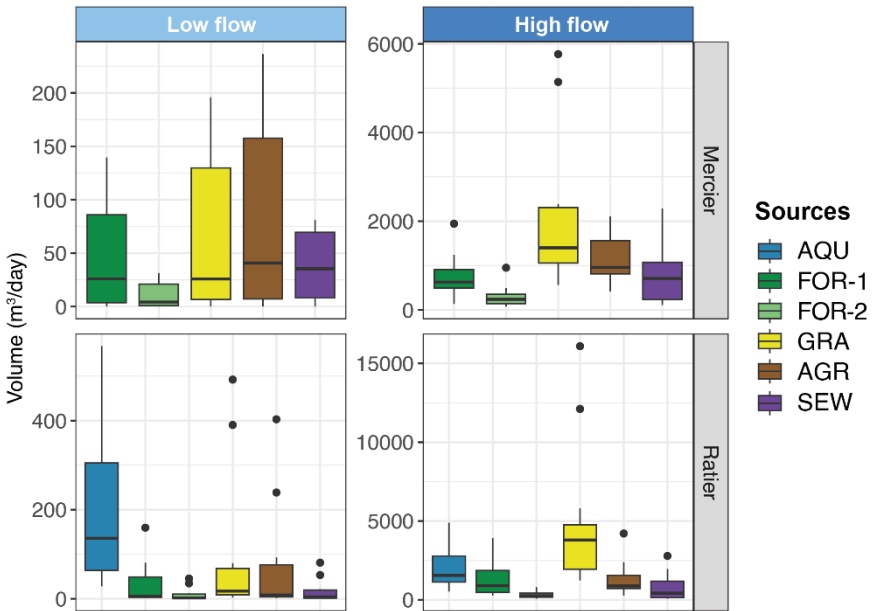
	06/03/19		07/03/19		07/03/19		07/03/19		07/03/19		07/03/19		07/03/19		07/03/19		07/03/19		07/03/19		07/03/19				
	23:15		00:15		01:15		02:15		03:15		04:15		05:15		06:15		07:15		08:15		09:15		10:15		
		Mean	sd																						
06/03/2019 - Mercier	<u>FOR</u> <u>1</u>	17	12	34	7	25	7	30	8	32	8	31	8	33	8	33	8	34	8	35	8	36	8	32	9
	<u>FOR</u> <u>2</u>	5	5	4	4	6	8	5	6	4	5	4	5	5	6	5	7	4	6	4	5	4	5	3	3
	<u>GRA</u>	31	11	20	5	26	8	27	7	15	6	12	6	16	6	17	7	19	7	19	7	19	7	11	5
	<u>AGR</u>	32	21	7	6	8	8	7	8	8	9	11	9	11	8	9	7	8	7	7	6	7	6	8	
	<u>URB</u>	0	0	5	6	3	4	5	6	5	7	5	7	5	6	5	6	7	6	8	6	8	7	10	
	<u>SEW</u>	16	4	15	3	11	2	13	3	19	3	19	3	17	3	18	3	18	3	19	4	18	4	21	4
	<u>SUR</u>	0	0	15	3	21	5	13	4	16	5	17	5	14	4	13	4	12	4	10	4	11	4	20	5
13/03/2023 - Mercier		<u>13/03/23</u>	<u>14/03/23</u>	<u>14/03/23</u>																					
			<u>18:37</u>	<u>19:07</u>	<u>19:37</u>	<u>20:07</u>	<u>20:37</u>	<u>21:07</u>	<u>21:37</u>	<u>22:07</u>	<u>22:37</u>	<u>23:07</u>	<u>23:37</u>	<u>00:07</u>											
		Mean	sd																						
	<u>FOR</u> <u>1</u>	13	11	6	5	14	12	5	5	6	6	9	8	8	7	7	6	4	4	4	3	5	5	6	6
	<u>FOR</u> <u>2</u>	3	3	14	6	12	9	43	19	36	18	27	15	23	13	23	13	25	14	26	15	26	15	22	13
	<u>GRA</u>	35	23	6	6	8	8	9	6	8	6	8	9	7	12	6	13	6	13	8	13	9	11	10	
	<u>AGR</u>	23	22	8	4	8	8	6	9	6	8	9	7	13	6	16	5	15	5	15	7	13	8	12	9
	<u>URB</u>	0	0	52	7	48	11	19	5	19	5	31	7	23	8	18	7	17	7	18	7	22	7	27	8
	<u>SEW</u>	26	5	7	3	5	3	2	1	2	1	5	2	11	4	14	4	15	4	14	4	15	4	15	4
	<u>SUR</u>	0	0	7	2	5	3	15	8	23	8	10	6	14	7	18	7	18	7	16	7	9	6	8	5
13/03/2023 - Ratiel		<u>13/03/23</u>	<u>14/03/23</u>																						
			<u>18:30</u>	<u>20:45</u>	<u>22:07</u>	<u>22:37</u>	<u>23:15</u>	<u>23:30</u>	<u>23:45</u>	<u>00:00</u>	<u>00:15</u>														
		Mean	sd																						
	<u>FOR</u> <u>1</u>	14	10	3	3	3	4	3	3	2	2	2	2	2	2	3	3	4	4						
	<u>FOR</u> <u>2</u>	7	6	2	2	2	2	2	2	1	2	1	2	1	2	2	3	2	3						
	<u>GRA</u>	13	11	21	6	21	9	18	7	20	8	19	8	21	8	22	8	22	8						
	<u>AGR</u>	9	8	7	4	6	6	9	7	5	5	5	5	6	6	10	8	10	8						
	<u>AQU</u>	44	11	1	1	1	1	1	1	1	1	1	1	1	1	1	1	1	1	1	1	1	1	1	
	<u>URB</u>	0	0	28	6	44	12	29	9	43	10	47	11	39	10	35	10	36	10						
	<u>SEW</u>	13	7	4	2	6	4	6	3	5	3	5	3	6	3	6	3	8	3						
	<u>SUR</u>	0	0	35	4	18	5	32	4	22	5	19	5	23	5	20	5	17	5						

Table A8 – Mean contributions and standard deviations of estimations obtained for the decomposition of streamwater samples collected during summer storm events in June 2022 and September 2022. The values correspond to the relative parts of flow for each time step as a percentage.

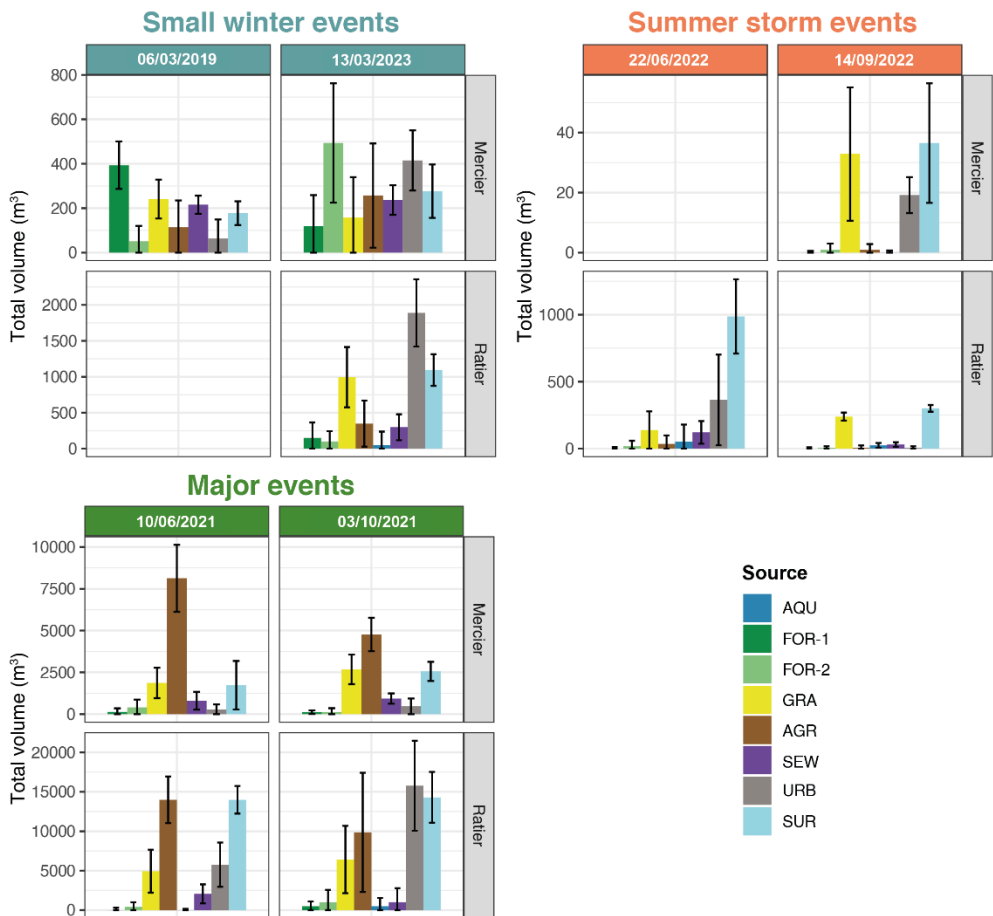
	22/06/22 15:07		22/06/22 15:37		22/06/22 16:07		22/06/22 16:37		22/06/22 17:07		22/06/22 17:37		22/06/22 18:07		22/06/22 18:37		22/06/22 19:07		22/06/22 19:37		22/06/22 20:07			
	Mean	sd	Mean	sd	Mean	sd	Mean	sd	Mean	sd	Mean	sd	Mean	sd										
22/06/2022 - Rattier	<u>FOR</u> 1	0	0	0	1	1	1	0	1	0	1	0	1	0	1	0	1	0	1	0	1	0	1	
	<u>FOR</u> 2	1	1	1	2	3	5	2	3	1	2	1	2	1	2	1	2	1	2	2	2	2	2	
	<u>GRA</u>	5	4	6	7	14	10	11	10	6	6	11	10	12	11	8	7	6	6	7	7	7	7	
	<u>AGR</u>	1	2	1	2	3	4	2	3	1	2	1	2	2	3	2	3	3	2	3	5	3	5	
	<u>AQU</u>	16	21	3	4	6	7	3	4	2	2	2	3	2	3	2	3	3	4	3	3	3	3	
	<u>URB</u>	48	34	34	26	23	17	21	17	19	15	17	14	17	14	17	13	26	19	23	18	24	18	
	<u>SEW</u>	8	8	6	5	6	4	5	4	4	3	3	3	4	3	5	3	12	7	10	6	10	6	
	<u>SUR</u>	20	9	48	23	44	15	56	17	66	15	64	17	61	16	65	13	48	15	52	15	51	17	
09/09/2022 - Mercier	<u>14/09/22 17:20</u>	<u>14/09/22 17:35</u>	<u>14/09/22 17:55</u>	<u>14/09/22 18:15</u>	<u>14/09/22 18:35</u>	<u>14/09/22 18:55</u>	<u>14/09/22 19:15</u>	<u>14/09/22 19:35</u>	<u>14/09/22 19:55</u>	<u>14/09/22 20:15</u>														
	Mean	sd	Mean	sd	Mean	sd	Mean	sd	Mean	sd	Mean	sd	Mean	sd										
	<u>FOR</u> 1	0	0	0	0	0	0	0	1	0	0	1	0	1	0	1	1	1	1	1	1	1	1	
	<u>FOR</u> 2	1	1	1	1	1	2	1	2	1	1	3	2	3	2	3	2	3	2	3	2	3	3	
	<u>GRA</u>	31	22	39	28	34	24	34	24	38	27	36	25	35	24	34	23	33	22	34	23			
	<u>AGR</u>	1	5	1	4	1	5	1	5	1	6	1	7	2	7	2	8	2	8	3	8			
	<u>URB</u>	33	1	17	1	22	1	22	1	19	2	22	2	25	2	27	3	30	3	29	4			
	<u>SEW</u>	1	0	0	0	0	0	0	1	0	1	1	1	1	1	1	1	1	1	1	1			
	<u>SUR</u>	32	22	42	28	42	24	41	23	40	24	38	21	35	20	34	19	32	17	31	18			
09/09/2022 - Rattier	-	-	-	-	-	-	-	-	-	-	-	-	-	-	-	-	-	-	-	-	-	-		
	14/09/22 16:35	14/09/22 16:55	14/09/22 17:15	14/09/22 17:35	14/09/22 17:55	14/09/22 18:15	14/09/22 18:35	14/09/22 18:55	14/09/22 19:15	14/09/22 19:35	14/09/22 19:55	14/09/22 20:15												
	Mean	sd	Mean	sd	Mean	sd	Mean	sd	Mean	sd	Mean	sd	Mean	sd										
	<u>FOR</u> 1	3	3	3	4	0	0	0	0	0	0	0	0	0	0	0	1	0	1	1	1	1	1	
	<u>FOR</u> 2	4	3	4	4	1	1	0	1	0	1	0	1	1	1	1	1	1	1	2	1	2	2	
	<u>GRA</u>	3	3	4	4	26	4	35	5	41	5	46	5	45	5	44	5	43	5	41	6	38	6	38
	<u>AGR</u>	5	4	6	6	2	2	1	1	1	1	1	1	1	1	1	2	2	2	2	3	3	4	
	<u>AQU</u>	72	5	70	5	40	3	4	2	4	2	3	1	4	2	5	2	7	2	10	2	12	2	
	<u>URB</u>	0	0	0	0	2	2	1	2	1	1	1	1	1	1	1	2	2	2	3	3	4		
	<u>SEW</u>	13	6	14	6	9	2	7	1	4	1	2	1	2	1	2	1	3	1	3	1	4	2	
	<u>SUR</u>	0	0	0	0	20	3	51	4	49	4	47	4	46	4	46	4	44	4	41	5	40	5	35

Table A9 – Mean contributions and standard deviations of estimations obtained for the decomposition of streamwater samples collected during major events in May 2021 and October 2021. The values correspond to the relative parts of flow for each time step as a percentage.

		10/05/21 09:45		10/05/21 10:45		10/05/21 11:45		10/05/21 12:45		10/05/21 13:45		10/05/21 14:45		10/05/21 15:45		10/05/21 16:45		10/05/21 17:45		10/05/21 18:45		10/05/21 19:45		10/05/21 20:45		
		Mean	sd																							
10/05/2021 - Mercier		<u>FOR 1</u>	1	1	2	3	1	2	1	2	1	1	1	1	1	1	1	1	1	1	2	1	1	1	1	1
		<u>FOR 2</u>	2	3	2	3	3	4	3	4	2	3	2	3	2	3	2	3	2	3	3	3	4	3	3	4
		<u>GRA</u>	10	4	7	5	9	6	9	6	8	6	10	7	11	7	14	7	12	7	17	8	19	9	19	9
		<u>AGR</u>	66	11	67	15	63	16	62	17	66	17	64	16	64	16	59	15	62	15	59	14	57	14	59	14
		<u>URB</u>	2	2	2	2	2	2	2	2	2	2	2	2	2	2	2	3	2	3	2	3	2	3	2	2
		<u>SEW</u>	6	3	7	4	5	4	5	4	4	4	4	4	4	4	5	4	7	4	6	4	7	4	7	4
		<u>SUR</u>	13	9	12	11	17	12	18	13	17	13	16	12	15	12	14	11	14	11	11	9	10	8	9	7
10/05/2021 - Rattier		10/05/21 10:15		10/05/21 11:15		10/05/21 12:15		10/05/21 13:15		10/05/21 14:15		10/05/21 15:15		10/05/21 16:15		10/05/21 17:15		10/05/21 18:15		10/05/21 19:15		10/05/21 20:15		10/05/21 21:15		
		Mean	sd																							
		<u>FOR 1</u>	0	0	1	1	1	1	1	1	0	1	0	1	0	1	0	1	0	1	0	1	0	1	1	1
		<u>FOR 2</u>	1	1	1	2	1	2	1	1	1	1	1	1	1	1	1	1	1	1	1	1	1	2	1	2
		<u>GRA</u>	10	4	11	6	11	6	10	6	10	6	11	7	9	6	10	6	11	7	13	8	13	8	15	9
		<u>AGR</u>	21	4	21	6	17	6	22	6	22	6	26	7	31	7	33	7	35	7	39	8	41	9	45	11
		<u>AQU</u>	0	0	0	0	0	1	0	0	1	0	0	0	0	0	0	0	0	0	0	0	0	0	0	
		<u>URB</u>	12	5	11	5	19	7	18	7	15	7	15	7	15	7	15	7	15	7	14	7	13	7	13	7
		<u>SEW</u>	4	2	4	2	5	3	5	3	5	3	5	3	4	3	5	3	4	3	5	3	5	3	6	4
		<u>SUR</u>	51	3	52	3	45	4	43	4	47	4	43	4	40	5	37	5	33	5	28	5	25	5	19	5
03/10/2021 - Mercier		03/10/21 14:37		03/10/21 16:07		03/10/21 17:37		03/10/21 19:07		03/10/21 20:37		03/10/21 22:07		03/10/21 23:37		04/10/21 01:07		04/10/21 02:37		04/10/21 04:07		04/10/21 05:37		04/10/21 07:07		
		Mean	sd																							
		<u>FOR 1</u>	1	1	0	0	0	1	0	1	0	1	1	1	0	1	1	1	1	1	1	1	1	1	1	1
		<u>FOR 2</u>	1	1	1	1	1	2	1	2	1	2	1	2	1	2	2	2	3	2	2	2	2	2	2	
		<u>GRA</u>	26	6	16	9	13	6	15	7	17	7	21	8	24	8	30	8	30	8	33	8	34	8	32	8
		<u>AGR</u>	40	6	33	8	47	8	47	9	43	9	45	9	44	9	39	9	38	9	36	9	33	9	33	9
		<u>URB</u>	4	3	2	2	2	3	3	3	3	3	3	3	3	4	4	6	5	6	5	6	7	6		
		<u>SEW</u>	9	2	2	2	2	1	5	2	6	2	5	2	6	3	10	3	13	3	13	3	14	3	15	3
		<u>SUR</u>	20	4	47	6	35	5	29	6	28	6	24	6	20	6	15	5	11	4	9	4	10	4	11	4
03/10/2021 - Rattier		03/10/21 14:37		03/10/21 16:07		03/10/21 17:37		03/10/21 19:07		03/10/21 20:37		03/10/21 22:07		03/10/21 23:37		04/10/21 01:07		04/10/21 02:37		04/10/21 04:07		04/10/21 05:37		04/10/21 07:07		
		Mean	sd																							
		<u>FOR 1</u>	1	1	0	1	1	1	1	1	1	1	1	1	1	1	1	1	1	1	1	1	1	1	2	1
		<u>FOR 2</u>	2	2	1	2	1	2	2	3	2	3	2	3	2	3	3	4	3	4	2	4	3	4	3	4
		<u>GRA</u>	10	5	9	7	13	10	13	9	11	8	13	9	12	8	12	8	14	9	12	9	16	10	14	10
		<u>AGR</u>	13	9	10	9	14	12	18	14	19	15	20	15	22	16	24	17	24	18	23	20	22	17	22	17
		<u>AQU</u>	2	6	0	1	1	1	1	1	1	1	1	1	1	1	1	1	1	1	2	1	2	1	2	
		<u>URB</u>	52	11	22	8	29	11	26	11	27	11	28	12	31	12	34	12	35	12	44	14	40	12	43	11
		<u>SEW</u>	5	7	1	1	1	1	2	2	2	2	2	2	3	3	4	3	5	4	4	5	5	5	5	
		<u>SUR</u>	16	4	56	6	40	8	39	7	38	7	34	7	30	7	24	7	19	7	14	7	13	6	11	6



947 **Figure A1 – Daily volume contributions in m^3 estimated for dry weather streamwater samples by the application of a biogeochemical**
948 **decomposition using a Bayesian mixing model for the Mercier and Ratier catchments. Contributions in terms of volume were**
949 **calculated based on the relative contributions for each source and the total flow for each sampled day in m^3 . Boxplots represent the**
950 **median contribution, interquartile range (1st and 3rd quartiles), minimum and maximum values. Low flow samples correspond to**
951 **a mean daily discharge lower than 20 L/s and high flow samples to a mean daily discharge higher than 20 L/s.**



953
954 **Figure A2 – Total volume contributions to the hydrological events sampled between March 2019 and March 2023 at the outlets of**
955 **the Mercier and Ratier catchments. Contributions in terms of volume were calculated based on the relative contributions from each**
956 **source and the total flow in m^3 . The contributions correspond to the mean of the results obtained for each samples decomposition**
957 **by the Bayesian mixing model approach. The error bars correspond to the mean of the standard deviation calculated from the sum**
958 **of the squares of the deviation. The events of 6 March 2019 at the Ratier station and 22 June 2022 at the Mercier station were not**
959 **collected.**

961 **Data availability**

962 Hydro-meteorological data and biogeochemical data at the catchment outlets during dry weather is available online at
963 <https://bdoh.irstea.fr/YZERON/station/V3015810> and <https://bdoh.irstea.fr/YZERON/station/V301502401>, respectively for
964 the Mercier and the Ratier station (<https://doi.org/10.57745/VVQ2X9>; <https://doi.org/10.17180/obs.yzeron>). Metadata relative
965 to the sampling of sources and of the catchment outlets are detailed at: <https://doi.org/10.57745/K3S9YV>. Biogeochemical
966 data of the sources and at the catchment outlets during hydrological events is available at <https://doi.org/10.57745/HQPIFQ>
967 for major parameters and dissolved metals, and at <https://doi.org/10.57745/IYJ2VE> for characteristics of DOM.

968 **Author contributions**

969 **OG**: Writing – original draft, Visualization, Methodology, Investigation, Formal analysis, Conceptualization. **FB**: Writing –
970 review & editing, Investigation, Methodology, Conceptualization. **MM**: Writing – review & editing, Investigation,
971 Methodology, Conceptualization. **BC**: Writing – review & editing, Investigation, Methodology. **NR**: Writing – review &
972 editing, Investigation, Methodology. **PD**: Writing – review & editing, Investigation, Methodology. **ADL**: Writing – review &
973 editing, Investigation, Methodology. **MC**: Writing – review & editing, Investigation, Methodology, Conceptualization,
974 Funding acquisition, Project administration.

975 **Declaration of competing interest**

976 The authors declare that they have no known competing financial interests or personal relationships that could have appeared
977 to influence the work reported in this paper.

978 **Acknowledgements**

979 Authors thanks Corinne Brosse-Quilgars, Lysiane Dherret, Loïc Richard, Aymeric Dabrin, Amandine Daval and Christelle
980 Margoum of the Aquatic Chemistry Laboratory team of RiverLy (INRAE), and Laurence Marjolet and B. Youenou of UMR
981 Ecologie Microbienne (VetAgro Sup) for the analysis of the samples, as well as M. Lagouy (INRAE, RiverLy) for field
982 sampling. We also thank the OTHU (Field Observatory in Urban Hydrology) and OZCAR (Critical Zone Observatories:
983 Research and Application) observatories for data provision. This work was carried out in the frame of a PhD, which was partly
984 funded by EUR H2O Lyon, and in the frame of the CHYPSTER research project partly funded by the French National Research
985 Agency (ANR-21-CE34-0013-01) and the IDESOC project granted by the ZABR – Rhone Basin LTSER within the Water
986 Agency RMC – RB LTSER funding agreement.

987

989 AFNOR. (2013). Standard method NF ISO 11352. Water Quality—Estimation of measurement uncertainty based on
990 validation and quality control data.

991 AFNOR. (2018). Standard method NF T90-210. Water quality—Protocol for the intial method performance assesment in a
992 laboratory.

993 Aussel, H., Bâcle, C. L., & Dornier, G. (2004). Le traitement des eaux usées. INRS.

994 Barthold, F. K., Wu, J., Vaché, K. B., Schneider, K., Frede, H.-G., & Breuer, L. (2010). Identification of geographic runoff
995 sources in a data sparse region : Hydrological processes and the limitations of tracer-based approaches.
996 *Hydrological Processes*, 24(16), 2313-2327. <https://doi.org/10.1002/hyp.7678>

997 Becouze-Lareure, C. (2010). Caractérisation et estimation des flux de substances prioritaires dans les rejets urbains par
998 temps de pluie sur deux bassins versants expérimentaux (p. 1 vol. (298 p.)) [Phd, Thèse de doctorat].
999 <http://www.theses.fr/2010ISAL0089>

1000 Begum, M. S., Park, H.-Y., Shin, H.-S., Lee, B.-J., & Hur, J. (2023). Separately tracking the sources of hydrophobic and
1001 hydrophilic dissolved organic matter during a storm event in an agricultural watershed. *Science of The Total
1002 Environment*, 873, 162347. <https://doi.org/10.1016/j.scitotenv.2023.162347>

1003 Benjamin, M. M. (2014). Water Chemistry : Second Edition. Waveland Press. [https://books.google.fr/books?id=dr-VBAAAQBAJ](https://books.google.fr/books?id=dr-
1004 VBAAAQBAJ)

1005 Bétemp, M. (2021). Diagnostic de l'occupation du sol et de l'utilisation des produits chimiques sur le bassin versant de
1006 l'Yzeron (Rhône) : Utilisation combinée d'enquêtes et de données cartographiques pour identifier les sources de
1007 contaminants et leur localisation. [Master]. Mémoire de Master, Université Grenobles Alpes, Laboratoire IGE
1008 Cermosem.

1009 Beven, K. (2012). Rainfall-runoff modelling : The primer, second edition (Vol. 457). John Wiley & Sons, Ltd.

1010 Birkel, C., & Soulsby, C. (2015). Advancing tracer-aided rainfall-runoff modelling : A review of progress, problems and
1011 unrealised potential. *Hydrological Processes*, 29(25), 5227-5240. <https://doi.org/10.1002/hyp.10594>

1012 Birkinshaw, S. J., O'Donnell, G., Glenis, V., & Kilsby, C. (2021). Improved hydrological modelling of urban catchments
1013 using runoff coefficients. *Journal of Hydrology*, 594, 125884. <https://doi.org/10.1016/j.jhydrol.2020.125884>

1014 Bomboi, M. T., & Hernandez, A. (1991). Hydrocarbons in urban runoff : Their contribution to thewastewaters. *Water
1015 Research*, 25(5), 557-565.

1016 Bouchali, R., Mandon, C., Danty - Berger, E., Géloën, A., Marjolet, L., Youenou, B., Pozzi, A. C. M., Vareilles, S., Galia,
1017 W., Kouyi, G. L., Toussaint, J.-Y., & Cournoyer, B. (2024). Runoff microbiome quality assessment of a city center
1018 rainwater harvesting zone shows a differentiation of pathogen loads according to human mobility patterns.
1019 *International Journal of Hygiene and Environmental Health*, 260, 114391.
1020 <https://doi.org/10.1016/j.ijheh.2024.114391>

1021 Boukra, A., Masson, M., Brosse, C., Sourzac, M., Parlanti, E., & Miège, C. (2023). Sampling terrigenous diffuse sources in
1022 watercourse : Influence of land use and hydrological conditions on dissolved organic matter characteristics. *Science
1023 of The Total Environment*, 872, 162104. <https://doi.org/10.1016/j.scitotenv.2023.162104>

1024 Braud, I., Branger, F., Chancibault, K., Jacqueminet, C., Breil, P., Chocat, B., Debionne, S., Dodane, C., Honegger, A.,
1025 Joliveau, T., Kermadi, S., Leblois, E., Lipeme Kouyi, G., Michel, K., Mosini, M. L., Renard, F., Rodriguez, F.,
1026 Sarrazin, B., Schmitt, L., ... Viallet, P. (2011). Assessing the vulnerability of PeriUrban rivers. Rapport scientifique
1027 final du projet AVuPUR (ANR-07-VULN-01) (p. 96) [Research Report]. IRSTEA. <https://hal.inrae.fr/hal-02596619>

1028 Braud, I., Breil, P., & Lagouy, M. (2018). Surveillance, prévision des crues et inondations dans le bassin de l'Yzeron : Etude
1029 de définition d'un système d'interprétation des relations entre la saturation des sols, les précipitations et les débits.
1030 Irstea.

1031 Bruijnzeel, L. A. (2004). Hydrological functions of tropical forests : Not seeing the soil for the trees? *Agriculture,
1032 Ecosystems & Environment*, 104(1), 185-228. <https://doi.org/10.1016/j.agee.2004.01.015>

1033 Burns, D. A., McDonnell, J., Hooper, R. P., Peters, N. E., Freer, J. E., Kendall, C., & Beven, K. (2001). Quantifying
1034 contributions to storm runoff through end-member mixing analysis and hydrologic measurements at the Panola
1035 Mountain research watershed (Georgia, USA). *Hydrological Processes*, 15(10), 1903-1924.
1036 <https://doi.org/10.1002/hyp.246>

1037 Cabral Nascimento, R., Jamil Maia, A., Jacques Agra Bezerra da Silva, Y., Farias Amorim, F., Williams Araújo do
1038 Nascimento, C., Tiecher, T., Evrard, O., Collins, A. L., Miranda Biondi, C., & Jacques Agra Bezerra da Silva, Y.
1039 (2023). Sediment source apportionment using geochemical composite signatures in a large and polluted river
1040 system with a semiarid-coastal interface, Brazil. *CATENA*, 220, 106710.
1041 <https://doi.org/10.1016/j.catena.2022.106710>

1042 Charters, F. J., Cochrane, T. A., & O'Sullivan, A. D. (2016). Untreated runoff quality from roof and road surfaces in a low
1043 intensity rainfall climate. *Science of The Total Environment*, 550, 265-272.
1044 <https://doi.org/10.1016/j.scitotenv.2016.01.093>

1045 Chocat, B., Krebs, P., Marsalek, J., Rauch, W., & Schilling, W. (2001). Urban drainage redefined : From stormwater
1046 removal to integrated management. *Water Science and Technology*, 43(5), 61-68.
1047 <https://doi.org/10.2166/wst.2001.0251>

1048 Christophersen, N., & Hooper, R. P. (1992). Multivariate analysis of stream water chemical data : The use of principal
1049 components analysis for the end-member mixing problem. *Water Resources Research*, 28(1), 99-107.
1050 <https://doi.org/10.1029/91WR02518>

1051 Christophersen, N., Neal, C., Hooper, R., Vogt, R., & Andersen, S. (1990). Modeling streamwater chemistry as a mixture of
1052 soil water end-members—A step towards second generation acidification models. *Journal of Hydrology*, 116,
1053 307-320. [https://doi.org/10.1016/0022-1694\(90\)90130-P](https://doi.org/10.1016/0022-1694(90)90130-P)

1054 Colin, Y., Bouchali, R., Marjolet, L., Marti, R., Vautrin, F., Voisin, J., Bourgeois, E., Rodriguez-Nava, V., Blaha, D.,
1055 Winiarski, T., Mermilliod-Blondin, F., & Cournoyer, B. (2020). Coalescence of bacterial groups originating from
1056 urban runoffs and artificial infiltration systems among aquifer microbiomes. *Hydrology and Earth System Sciences*,
1057 24(9), 4257-4273. <https://doi.org/10.5194/hess-24-4257-2020>

1058 Collins, A. L., Pulley, S., Foster, I. D. L., Gellis, A., Porto, P., & Horowitz, A. J. (2017). Sediment source fingerprinting as
1059 an aid to catchment management : A review of the current state of knowledge and a methodological decision-tree
1060 for end-users. *Journal of Environmental Management*, 194, 86-108. <https://doi.org/10.1016/j.jenvman.2016.09.075>

1061 Collins, A. L., Walling, D. E., & Leeks, G. J. L. (1997). Use of the geochemical record preserved in floodplain deposits to
1062 reconstruct recent changes in river basin sediment sources. *Geomorphology*, 19(1), 151-167.
1063 [https://doi.org/10.1016/S0169-555X\(96\)00044-X](https://doi.org/10.1016/S0169-555X(96)00044-X)

1064 Cooper, D. M., Jenkins, A., Skeffington, R., & Gannon, B. (2000). Catchment-scale simulation of stream water chemistry by
1065 spatial mixing : Theory and application. *Journal of Hydrology*, 233(1-4), 121-137. [https://doi.org/10.1016/S0022-1694\(00\)00230-4](https://doi.org/10.1016/S0022-1694(00)00230-4)

1066 Coquery, M., Pomies, M., Martin Ruel, S., Budzinski, H., Miege, C., Esperanza, M., Soulier, C., & Choubert, J. M. (2011).
1067 Mesurer les micropolluants dans les eaux usées brutes et traitées. Protocoles et résultats pour l'analyse des
1068 concentrations et des flux. *Techniques Sciences Méthodes*, 1-2, 25-43.

1069 Cristiano, E., ten Veldhuis, M.-C., & van de Giesen, N. (2017). Spatial and temporal variability of rainfall and their effects
1070 on hydrological response in urban areas – a review. *Hydrology and Earth System Sciences*, 21(7), 3859-3878.
1071 <https://doi.org/10.5194/hess-21-3859-2017>

1072 David, L., Elmi, S., & Féraud, J. (1979). Carte géologique de la france au 1/50 000—Lyon. Feuille XXX-31. BRGM,
1073 Service Géologique National, 41.

1074 Deletic, A., & Orr, D. W. (2005). Pollution buildup on road surfaces. *Journal of Environmental Engineering*, 131(1), 49-59.
1075 [https://doi.org/10.1061/\(ASCE\)0733-9372\(2005\)131:1\(49\)](https://doi.org/10.1061/(ASCE)0733-9372(2005)131:1(49))

1076 Delfour, J., Dufour, E., Feybesse, J. I., Johan, V., Kerrien, Y., Lardeaux, J. M., Lemière, B., Mouterde, R., & Tegyey, M.
1077 (1989). Notice explicative, carte géol. France (1/50000), feuille tarare (697). Orléans: Bureau de recherches
1078 géologiques et minières, 120.

1079 Dubois, V., Falipou, E., & Boutin, C. (2022). Quantification and qualification of the urban domestic pollution discharged per
1080 household and per resident. *Water Science and Technology*, 85(5), 1484-1499.
1081 <https://doi.org/10.2166/wst.2022.064>

1082 Dunn, O. J. (1964). Multiple comparisons using rank sums. *Technometrics : a journal of statistics for the physical, chemical,
1083 and engineering sciences*, 6(3), 241-252. <https://doi.org/10.2307/1266041>

1084 El Azzi, D., Probst, J. L., Teisserenc, R., Merlina, G., Baqué, D., Julien, F., Payre-Suc, V., & Guiresse, M. (2016). Trace
1085 element and pesticide dynamics during a flood event in the save agricultural watershed : Soil-river transfer
1086

1087 pathways and controlling factors. *Water, Air, and Soil Pollution*, 227(12). <https://doi.org/10.1007/s11270-016-3144-0>

1088 Eme, C., & Boutin, C. (2015). Composition des eaux usées domestiques par source d'émission à l'échelle de l'habitation.
1089 Etude bibliographique (p. 90) [Research Report]. irstea. <https://hal.inrae.fr/hal-02605815>

1090 Emmanuel, I., Andrieu, H., Flahaut, B., & Furusho, C. (2012). Influence of rainfall spatial variability on rainfall runoff
1091 modelling : Case study on a peri-urban catchment.

1092 Fines, R. W., Stone, M., Webster, K. L., Leach, J. A., Buttle, J. M., Emelko, M. B., & Collins, A. L. (2023). Evaluation of
1093 Legacy Forest Harvesting Impacts on Dominant Stream Water Sources and Implications for Water Quality Using
1094 End Member Mixing Analysis. *WATER*, 15(15). <https://doi.org/10.3390/w15152825>

1095 Froger, C., Quantin, C., Bordier, L., Monvoisin, G., Evrard, O., & Ayrault, S. (2020). Quantification of spatial and temporal
1096 variations in trace element fluxes originating from urban areas at the catchment scale. *Journal of Soils and*
1097 *Sediments*, 20(11), 4055-4069. <https://doi.org/10.1007/s11368-020-02766-1>

1098 Fröhlich, H. L., Breuer, L., Frede, H.-G., Huisman, J. A., & Vaché, K. B. (2008). Water source characterization through
1099 spatiotemporal patterns of major, minor and trace element stream concentrations in a complex, mesoscale German
1100 catchment. *Hydrological Processes*, 22(12), 2028-2043. <https://doi.org/10.1002/hyp.6804>

1101 Fröhlich, H. L., Breuer, L., Vaché, K. B., & Frede, H.-G. (2008). Inferring the effect of catchment complexity on mesoscale
1102 hydrologic response. *Water Resources Research*, 44(9). <https://doi.org/10.1029/2007WR006207>

1103 Giri, S., & Qiu, Z. (2016). Understanding the relationship of land uses and water quality in Twenty First Century : A review.
1104 *Journal of Environmental Management*, 173, 41-48. <https://doi.org/10.1016/j.jenvman.2016.02.029>

1105 Gnouma, R. (2006). Aide à la calibration d'un modèle hydrologique distribué au moyen d'une analyse des processus
1106 hydrologiques : Application au bassin versant de l'Yzeron (p. 412) [Phd, Thèse de doctorat, INSA Lyon].
1107 <https://hal.inrae.fr/tel-02588466>

1108 Gonzales, A. L., Nonner, J., Heijkers, J., & Uhlenbrook, S. (2009). Comparison of different base flow separation methods in
1109 a lowland catchment. *Hydrology and Earth System Sciences*, 13(11), 2055-2068. <https://doi.org/10.5194/hess-13-2055-2009>

1110 Goutaland, D. (2009). Programme ANR AVuPUR - Prospection géophysique par panneau électrique de trois parcelles d'un
1111 sous-bassin versant de l'Yzeron. CETE de Lyon.

1112 Grandjouan, O. (2024). Apports de la biogéochimie pour l'évaluation d'un modèle hydrologique distribué en milieu péri-
1113 urbain [Phd]. Thèse de doctorat, INRAE.

1114 Grandjouan, O., Branger, F., Masson, M., Cournoyer, B., & Coquery, M. (2023). Identification and estimation of
1115 hydrological contributions in a mixed land-use catchment based on a simple biogeochemical and hydro-
1116 meteorological dataset. *Hydrological Processes*, 37(12), e15035. <https://doi.org/10.1002/hyp.15035>

1117 Helms, J. R., Stubbins, A., Ritchie, J. D., Minor, E. C., Kieber, D. J., & Mopper, K. (2008). Absorption spectral slopes and
1118 slope ratios as indicators of molecular weight, source, and photobleaching of chromophoric dissolved organic
1119 matter. *Limnology and Oceanography*, 53(3), 955-969. <https://doi.org/10.4319/lo.2008.53.3.0955>

1120 Iorgulescu, I., Beven, K. J., & Musy, A. (2005). Data-based modelling of runoff and chemical tracer concentrations in the
1121 Haute-Mentue research catchment (Switzerland). *Hydrological Processes*, 19(13), 2557-2573.
1122 <https://doi.org/10.1002/hyp.5731>

1123 Jacqueminet, C., Kermadi, S., Michel, K., Béal, D., Gagnage, M., Branger, F., Jankowfsky, S., & Braud, I. (2013). Land
1124 cover mapping using aerial and VHR satellite images for distributed hydrological modelling of periurban
1125 catchments : Application to the Yzeron catchment (Lyon, France). *Journal of Hydrology*, 485, 68-83.
1126 <https://doi.org/10.1016/j.jhydrol.2013.01.028>

1127 James, R., Amasi, A. I., Wynants, M., Nobert, J., Mtei, K. M., & Njau, K. (2023). Tracing the dominant sources of sediment
1128 flowing towards Lake Victoria using geochemical tracers and a Bayesian mixing model. *Journal of Soils and*
1129 *Sediments*, 23(3), 1568-1580. <https://doi.org/10.1007/s11368-023-03440-y>

1130 Jankowfsky, S. (2011). Understanding and modelling of hydrological processes in small peri-urban catchments using an
1131 object-oriented and modular distributed approach Application to the Chaudanne and Mercier sub-catchments
1132 (Yzeron catchment, France) (p. 331) [Theses, Thèse de doctorat, spécialité Océan, Atmosphère, Hydrologie, Ecole
1133 Doctorale Terre Univers Environnement, Université de Grenoble]. <https://hal.inrae.fr/tel-02596792>

1134

1135

1136 Kaown, D., Koh, D.-C., Mayer, B., Mahlknecht, J., Ju, Y., Rhee, S.-K., Kim, J.-H., Park, D. K., Park, I., Lee, H.-L., Yoon,
1137 Y.-Y., & Lee, K.-K. (2023). Estimation of nutrient sources and fate in groundwater near a large weir-regulated river
1138 using multiple isotopes and microbial signatures. *Journal of Hazardous Materials*, 446, 130703.
1139 <https://doi.org/10.1016/j.jhazmat.2022.130703>

1140 Kermadi, S., Braud, I., Jacqueminet, C., Branger, F., Renard, F., & Michel, K. (2012). Quels liens entre climatologie,
1141 occupation des sols et inondations dans le bassin versant de l'Yzeron (ouest Lyonnais) ? Apport de l'analyse
1142 conjointe de données hydroclimatiques et d'images satellitaires très haute résolution. *Climatologie*, 9, 83.

1143 Klages, M. G., & Hsieh, Y. P. (1975). Suspended Solids Carried by the Gallatin River of Southwestern Montana : II. Using
1144 Mineralogy for Inferring Sources. *Journal of Environmental Quality*, 4(1), 68-73.
1145 <https://doi.org/10.2134/jeq1975.00472425000400010016x>

1146 Kruskal, W. H., & Wallis, W. A. (1952). Use of ranks in one-criterion variance analysis. *Journal of the American Statistical
1147 Association*, 47(260), 583-621. <https://doi.org/10.2307/2280779>

1148 Kuhlemann, L.-M., Tetzlaff, D., & Soulsby, C. (2021). Spatio-temporal variations in stable isotopes in peri-urban
1149 catchments : A preliminary assessment of potential and challenges in assessing streamflow sources. *Journal of
1150 Hydrology*, 600, 126685. <https://doi.org/10.1016/j.jhydrol.2021.126685>

1151 Kumar, N., Ganguly, A., Biswal, K., Keesari, T., Pandey, A., & Deshpande, R. D. (2024). Relative contribution from
1152 different water sources to supraglacial runoff in western Himalaya. *Journal of Hydrology*, 635, 131137.
1153 <https://doi.org/10.1016/j.jhydrol.2024.131137>

1154 Labbas, M. (2014). Modélisation hydrologique de bassins versants périurbains et influence de l'occupation du sol et de la
1155 gestion des eaux pluviales. Application au bassin de l'Yzeron (130 km²) [Phd]. Thèse de doctorat, Université
1156 Grenoble Alpes.

1157 Lachassagne, P., Dewandel, B., & Wyns, R. (2021). Review : Hydrogeology of weathered crystalline/hard-rock aquifers—
1158 guidelines for the operational survey and management of their groundwater resources. *Hydrogeology Journal*,
1159 29(8), 2561-2594. <https://doi.org/10.1007/s10040-021-02339-7>

1160 Ladouche, B., Probst, A., Viville, D., Idir, S., Baqué, D., Loubet, M., Probst, J.-L., & Bariac, T. (2001). Hydrograph
1161 separation using isotopic, chemical and hydrological approaches (Strengbach catchment, France). *Journal of
1162 Hydrology*, 242(3-4), 255-274. [https://doi.org/10.1016/S0022-1694\(00\)00391-7](https://doi.org/10.1016/S0022-1694(00)00391-7)

1163 Lafont, M., Vivier, A., Nogueira, S., Namour, P., & Breil, P. (2006). Surface and hyporheic oligochaete assemblages in a
1164 french suburban stream. *Hydrobiologia*, 564(1), 183-193. <https://doi.org/10.1007/s10750-005-1718-8>

1165 Lagouy, M., Branger, F., & Breil, P. (2022). Rainfall monitoring on the Yzeron catchment since 1997 [Jeu de données].
1166 Recherche Data Gouv. <https://doi.org/10.57745/VVQ2X9>

1167 Lamprea, K., & Ruban, V. (2011). Pollutant concentrations and fluxes in both stormwater and wastewater at the outlet of
1168 two urban watersheds in Nantes (France). *Urban Water Journal*, 8(4), 219-231.
1169 <https://doi.org/10.1080/1573062X.2011.596211>

1170 Langlois, J. L., & Mehuys, G. R. (2003). Intra-storm study of solute chemical composition of overland flow water in two
1171 agricultural fields. *Journal of Environmental Quality*, 32(6), 2301-2310. <https://doi.org/10.2134/jeq2003.2301>

1172 Le, H. T., Pommier, T., Ribolzi, O., Soulileuth, B., Huon, S., Silvera, N., & Rochelle-Newall, E. (2022). Overland flow
1173 during a storm event strongly affects stream water chemistry and bacterial community structure. *Aquatic Sciences -
1174 Research Across Boundaries*, 84(1), 7. <https://doi.org/10.1007/s00027-021-00839-y>

1175 Li, P., & Hur, J. (2017). Utilization of UV-Vis spectroscopy and related data analyses for dissolved organic matter (DOM)
1176 studies : A review. *Critical Reviews in Environmental Science and Technology*, 47(3), 131-154.
1177 <https://doi.org/10.1080/10643389.2017.1309186>

1178 Lin, B., An, X., Zhao, C., Gao, Y., Liu, Y., Qiu, B., Qi, F., & Sun, D. (2024). Analysis of urban composite non-point source
1179 pollution characteristics and its contribution to river DOM based on EEMs and FT-ICR MS. *Water Research*, 266,
1180 122406. <https://doi.org/10.1016/j.watres.2024.122406>

1181 Liu, W.-R., Zeng, D., She, L., Su, W.-X., He, D.-C., Wu, G.-Y., Ma, X.-R., Jiang, S., Jiang, C.-H., & Ying, G.-G. (2020).
1182 Comparisons of pollution characteristics, emission situations, and mass loads for heavy metals in the manures of
1183 different livestock and poultry in China. In *Science of the Total Environment* (Vol. 734).
1184 <https://doi.org/10.1016/j.scitotenv.2020.139023>

1185 Liu, Y., Walling, D. E., Yang, M., & Zhang, F. (2023). Sediment source fingerprinting and the temporal variability of source
1186 contributions. *Journal of Environmental Management*, 338, 117835. <https://doi.org/10.1016/j.jenvman.2023.117835>

1187 Madani, E. M., Jansson, P. E., & Babelon, I. (2017). Differences in water balance between grassland and forest watersheds
1188 using long-term data, derived using the CoupModel. *Hydrology Research*, 49(1), 72-89.
<https://doi.org/10.2166/nh.2017.154>

1189 Marti, R., Ribun, S., Aubin, J.-B., Colinon, C., Petit, S., Marjollet, L., Gourmelon, M., Schmitt, L., Breil, P., Cottet, M., &
1190 Cournoyer, B. (2017). Human-driven microbiological contamination of benthic and hyporheic sediments of an
1191 intermittent peri-urban river assessed from MST and 16S rRNA genetic structure analyses. *Frontiers in*
1192 *Microbiology*, 8, 19. <https://doi.org/10.3389/fmicb.2017.00019>

1193 Martins, J., Coquery, M., Robinet, N., Nord, G., Duwig, C., Legout, C., Morel, M. C., Spadini, L., Hachgenei, N., Némery,
1194 J., Mao, P., Margoum, C., Miege, C., Daval, A., Mathon, B., & Liger, L. (2019). Origine et devenir des
1195 contaminants PHARMAcétiques dans les Bassins Versants agricoles. Le cas de la Claduègne (Ardèche).
1196 PHARMA-BV (p. 2). <https://hal.inrae.fr/hal-02609731>

1197 Masson, M., Grandjouan, O., Branger, F., Brosse, C., Dherret, L., Lagouy, M., Richard, L., & Coquery, M. (2025a).
1198 Analyses de paramètres majeurs et métaux dissous dans les échantillons de sources des bassins versants du Ratier et
1199 du Mercier (Lyon, France) [Jeu de données]. *Recherche Data Gouv*. <https://doi.org/10.57745/HQPIFQ>

1200 Masson, M., Grandjouan, O., Branger, F., Brosse, C., Dherret, L., Lagouy, M., Richard, L., & Coquery, M. (2025b).
1201 Analyses des indicateurs optiques de la matière organique dissoute mesurés dans les échantillons de sources des
1202 bassins versants du Ratier et du Mercier (Lyon, France) [Jeu de données]. *Recherche Data Gouv*.
1203 <https://doi.org/10.57745/IYJ2VE>

1204 McDonnell, J. J., Spence, C., Karran, D. J., van Meerveld, H. J. (Ilja), & Harman, C. J. (2021). Fill-and-Spill : A Process
1205 Description of Runoff Generation at the Scale of the Beholder. *Water Resources Research*, 57(5), e2020WR027514.
1206 <https://doi.org/10.1029/2020WR027514>

1207 McElmurry, S. P., Long, D. T., & Voice, T. C. (2014). Stormwater dissolved organic matter : Influence of land cover and
1208 environmental factors. *Environmental Science and Technology*, 48(1), 45-53. <https://doi.org/10.1021/es402664t>

1209 Mejía, A. I., & Moglen, G. E. (2010). Impact of the spatial distribution of imperviousness on the hydrologic response of an
1210 urbanizing basin. *Hydrological Processes*, 24(23), 3359-3373. <https://doi.org/10.1002/hyp.7755>

1211 Motha, J. A., Wallbrink, P. J., Hairsine, P. B., & Grayson, R. B. (2003). Determining the sources of suspended sediment in a
1212 forested catchment in southeastern Australia. *Water Resources Research*, 39(3).
1213 <https://doi.org/10.1029/2001WR000794>

1214 Nguyen, H., Peche, A., & Venohr, M. (2021). Modelling Of Sewer Exfiltration To Groundwater In Urban Wastewater
1215 Systems : A Critical Review. *Journal of Hydrology*, 126130. <https://doi.org/10.1016/j.jhydrol.2021.126130>

1216 Omogbehin, M. H., & Oluwatimilehin, I. A. (2022). Changes of water chemistry from rainfall to stream flow in Obagbile
1217 Catchment, Southwest Nigeria. *Regional Sustainability*, 3(2), 170-181. <https://doi.org/10.1016/j.regsus.2022.07.006>

1218 Penuelas, J., Coello, F., & Sardans, J. (2023). A better use of fertilizers is needed for global food security and environmental
1219 sustainability. *Agriculture & Food Security*, 12(1), 5. <https://doi.org/10.1186/s40066-023-00409-5>

1220 Peuravuori, J., & Pihlaja, K. (1997). Molecular size distribution and spectroscopic properties of aquatic humic substances.
1221 *Analytica Chimica Acta*, 337(2), 133-149. [https://doi.org/10.1016/S0003-2670\(96\)00412-6](https://doi.org/10.1016/S0003-2670(96)00412-6)

1222 Pozzi, A. C. M., Petit, S., Marjollet, L., Youenou, B., Lagouy, M., Namour, P., Schmitt, L., Navratil, O., Breil, P., Branger,
1223 F., & Cournoyer, B. (2024). Ecological assessment of combined sewer overflow management practices through the
1224 analysis of benthic and hyporheic sediment bacterial assemblages from an intermittent stream. *Science of The Total*
1225 *Environment*, 907, 167854. <https://doi.org/10.1016/j.scitotenv.2023.167854>

1226 Rai, S. P., Singh, D., Jacob, N., Rawat, Y. S., Arora, M., & BhishmKumar. (2019). Identifying contribution of snowmelt and
1227 glacier melt to the Bhagirathi River (Upper Ganga) near snout of the Gangotri Glacier using environmental
1228 isotopes. *CATENA*, 173, 339-351. <https://doi.org/10.1016/j.catena.2018.10.031>

1229 Ramon, R. (2021). Quantifying sediment source contributions in contrasted agricultural catchments (Uruguay River,
1230 Southern Brazil) (Theses 2021UPASJ009, Thèse de doctorat, Université Paris-Saclay ; Universidade Federal do Rio
1231 Grande do Sul (Porto Alegre, Brésil)). <https://theses.hal.science/tel-03434617>

1232 Robinson, M., & Dupeyrat, A. (2005). Effects of commercial timber harvesting on streamflow regimes in the Plynlimon
1233 catchments, mid-Wales. *Hydrological Processes*, 19(6), 1213-1226. <https://doi.org/10.1002/hyp.5561>

1234

1235 Sandin, M., Piikki, K., Jarvis, N., Larsbo, M., Bishop, K., & Kreuger, J. (2018). Spatial and temporal patterns of pesticide
1236 concentrations in streamflow, drainage and runoff in a small Swedish agricultural catchment. *The Science of the*
1237 *Total Environment*, 610-611, 623-634. <https://doi.org/10.1016/j.scitotenv.2017.08.068>

1238 Sanisaca, L. E. G., Gellis, A. C., & Lorenz, D. L. (2017). Determining the sources of fine-grained sediment using the
1239 *Sediment Source Assessment Tool (Sed_SAT)*. In *Open-File Report* (p. 116). <https://doi.org/10.3133/ofr20171062>

1240 Sarrazin, B. (2012). MNT et observations multi-locales du réseau de drainage d'un petit bassin versant rural dans une
1241 perspective d'aide à la modélisation spatialisée (Theses 2012GRENU042, Thèse de doctorat, Université Grenoble
1242 Alpes; p. 283). <https://tel.archives-ouvertes.fr/tel-01548105>

1243 Shi, M.-M., Wang, X.-M., Chen, Q., Han, B.-H., Zhou, B.-R., Xiao, J.-S., & Xiao, H.-B. (2021). Responses of soil moisture
1244 to precipitation and infiltration in dry and wet alpine grassland ecosystems. In *Acta Prataculturae Sinica* (Vol. 30,
1245 Numéro 12, p. 49-58). <https://doi.org/10.11686/cyxb2020436>

1246 Simpson, I. M., Winston, R. J., & Dorsey, J. D. (2023). Monitoring the effects of urban and forested land uses on runoff
1247 quality : Implications for improved stormwater management. *Science of The Total Environment*, 862, 160827.
1248 <https://doi.org/10.1016/j.scitotenv.2022.160827>

1249 Singh, S. K., & Stenger, R. (2018). Indirect methods to elucidate water flows and contaminant transfer pathways through
1250 meso-scale catchments – A review. *Environmental Processes*, 5(4), 683-706. <https://doi.org/10.1007/s40710-018-0331-6>

1251 Spence, C., & Woo, M. (2003). Hydrology of subarctic Canadian shield : Soil-filled valleys. *Journal of Hydrology*, 279(1),
1252 151-166. [https://doi.org/10.1016/S0022-1694\(03\)00175-6](https://doi.org/10.1016/S0022-1694(03)00175-6)

1253 Stock, B. C., Jackson, A. L., Ward, E. J., Parnell, A. C., Phillips, D. L., & Semmens, B. X. (2018). Analyzing mixing
1254 systems using a new generation of Bayesian tracer mixing models. *PeerJ*, 6(e5096).

1255 Sun, Z.-X., Cui, J.-F., Cheng, J.-H., & Tang, X.-Y. (2024). A novel tool for tracing water sources of streamflow in a mixed
1256 land-use catchment. *Science of The Total Environment*, 912, 168800.
1257 <https://doi.org/10.1016/j.scitotenv.2023.168800>

1258 Tardy, Y., Bustillo, V., & Boeglin, J.-L. (2004). Geochemistry applied to the watershed survey : Hydrograph separation,
1259 erosion and soil dynamics. A case study : The basin of the Niger River, Africa. *Applied Geochemistry*, 19(4),
1260 469-518. <https://doi.org/10.1016/j.apgeochem.2003.07.003>

1261 Thorndike, R. L. (1953). Who belongs in the family? *Psychometrika*, 18(4), 267-276. <https://doi.org/10.1007/BF02289263>

1262 Tiecher, T., Caner, L., Minella, J. P. G., & dos Santos, D. R. (2015). Combining visible-based-color parameters and
1263 geochemical tracers to improve sediment source discrimination and apportionment. *Science of The Total
1264 Environment*, 527-528, 135-149. <https://doi.org/10.1016/j.scitotenv.2015.04.103>

1265 Tran, N. H., Reinhard, M., Khan, E., Chen, H., Nguyen, V. T., Li, Y., Goh, S. G., Nguyen, Q. B., Saeidi, N., & Gin, K. Y.-H.
1266 (2019). Emerging contaminants in wastewater, stormwater runoff, and surface water : Application as chemical
1267 markers for diffuse sources. *Science of The Total Environment*, 676, 252-267.
1268 <https://doi.org/10.1016/j.scitotenv.2019.04.160>

1269 Tromp-van Meerveld, H. J., & McDonnell, J. (2006). Threshold relations in subsurface stormflow : 2. The fill and spill
1270 hypothesis. *Water Resources Research*, 42(2). <https://doi.org/10.1029/2004WR003800>

1271 Uber, M., Legout, C., Nord, G., Crouzet, C., Demory, F., & Poulenard, J. (2019). Comparing alternative tracing
1272 measurements and mixing models to fingerprint suspended sediment sources in a mesoscale Mediterranean
1273 catchment. *Journal of Soils and Sediments*, 19(9), 3255-3273. <https://doi.org/10.1007/s11368-019-02270-1>

1274 Vale, S., Swales, A., Smith, H. G., Olsen, G., & Woodward, B. (2022). Impacts of tracer type, tracer selection, and source
1275 dominance on source apportionment with sediment fingerprinting. *Science of The Total Environment*, 831, 154832.
1276 <https://doi.org/10.1016/j.scitotenv.2022.154832>

1277 Verseveld, W. J. van, McDonnell, J. J., & Lajtha, K. (2008). A mechanistic assessment of nutrient flushing at the catchment
1278 scale. *Journal of Hydrology*, 358(3), 268-287. <https://doi.org/10.1016/j.jhydrol.2008.06.009>

1279 Vian, J.-F. (2019). Agriculture biologique et qualité de l'eau. Etat des lieux des forces et faiblesses des systèmes de
1280 production conduits en AB. ISARA Lyon.

1281 Walsh, C. J., Roy, A. H., Feminella, J. W., Cottingham, P. D., Groffman, P. M., & Morgan, R. P. (2005). The urban stream
1282 syndrome : Current knowledge and the search for a cure. *Journal of the North American Benthological Society*,
1283 24(3), 706-723. <https://doi.org/10.1899/04-028.1>

1285 Wang, F., Liu, L., Xu, W., Li, Y., Ruan, Q., & Cao, W. (2024). Multiple stable isotopic approaches for tracing nitrate
1286 contamination sources : Implications for nitrogen management in complex watersheds. *Ecotoxicology and*
1287 *Environmental Safety*, 269, 115822. <https://doi.org/10.1016/j.ecoenv.2023.115822>

1288 Wang, Y.-H., Zhang, P., He, C., Yu, J.-C., Shi, Q., Dahlgren, R. A., Spencer, R. G. M., Yang, Z.-B., & Wang, J.-J. (2023).
1289 Molecular signatures of soil-derived dissolved organic matter constrained by mineral weathering. *Fundamental*
1290 *Research*, 3(3), 377-383. <https://doi.org/10.1016/j.fmre.2022.01.032>

1291 Wellington, B. I., & Driscoll, C. T. (2004). The episodic acidification of a stream with elevated concentrations of dissolved
1292 organic carbon. *Hydrological Processes*, 18(14), 2663-2680. <https://doi.org/10.1002/hyp.5574>

1293 White, A. F., Bullen, T. D., Vivit, D. V., Schulz, M. S., & Clow, D. W. (1999). The role of disseminated calcite in the
1294 chemical weathering of granitoid rocks. *Geochimica et Cosmochimica Acta*, 63(13), 1939-1953.
1295 [https://doi.org/10.1016/S0016-7037\(99\)00082-4](https://doi.org/10.1016/S0016-7037(99)00082-4)

1296 Wilkinson, S. N., Hancock, G. J., Bartley, R., Hawdon, A. A., & Keen, R. J. (2013). Using sediment tracing to assess
1297 processes and spatial patterns of erosion in grazed rangelands, Burdekin River basin, Australia. *Agriculture,*
1298 *Ecosystems and Environment*, 180, 90-102. <https://doi.org/10.1016/j.agee.2012.02.002>

1299 Yokel, J., & Delistraty, D. A. (2003). Arsenic, lead, and other trace elements in soils contaminated with pesticide residues at
1300 the Hanford site (USA). *Environmental toxicology*, 18(2), 104-114. <https://doi.org/10.1002/tox.10106>

1301